12-2008

Analysis of Effectiveness of Bridges with Partial Isolation

Wenying Hu
Utah State University

ANALYSIS OF EFFECTIVENESS OF BRIDGES WITH PARTIAL ISOLATION

by

Wenying Hu

A thesis submitted in partial fulfillment
of the requirements for the degree

of

MASTER OF SCIENCE

in

Civil and Environmental Engineering

Approved:

Keri L. Ryan Major Professor	YangQuan Chen Committee Member
Marvin W. Halling Committee Member	Byron R. Burnham Dean of Graduate Studies

UTAH STATE UNIVERSITY
Logan, Utah

2008

ABSTRACT

Analysis of the Effectiveness of Bridges with Partial Isolation

by

Wenying Hu, Master of Science

Utah Sate University, 2008

Major Professor: Dr. Keri L. Ryan
Department: Civil and Environmental Engineering

A special class of seismically isolated bridges shares a common feature in that both ends of the superstructure are restrained and isolators over the columns of bridge uncouple the superstructure from the ground motions. They are defined as partial isolation bridges. From measured acceleration responses, effectiveness of full seismic isolation had been confirmed widely. However, the seismic isolation behavior in the partial isolation has not been widely observed.

The effectiveness of partial isolation is evaluated in this study. The static design procedures for linear and nonlinear partially isolated bridges are developed. Results from the static analysis of linear and nonlinear partially isolated bridges, compared with conventional and fully isolated bridges, demonstrate that the effectiveness of nonlinear partial isolation is close to full isolation for reducing the yield force and displacement of the columns in some parameter ranges. However, increased seismic demands on the abutment displacement in the bridge are observed. Nonlinear time history analyses of the different bridge models under earthquake excitations are carried out to investigate the

accuracy of the design procedure for nonlinear partial isolation. In addition, an example shows the application of nonlinear partial isolation to a practical bridge.

(70 pages)

ACKNOWLEDGMENTS

First I would like to take the opportunity to thank my major professor, Dr. Keri L. Ryan, for all her valuable support towards my education. She has encouraged me and guided me towards exploring my skills as a researcher. She has worked with me with great patience and supported me by all means possible. I would like to thank my committee members, Dr. Marvin W. Halling and Dr. Yangquan Chen, for all the academic support and the contributions they have extended towards my education and for guiding me through my thesis with their inspirational insights.

Further, I would like to express my gratitude towards my family members for their love, warmth, and affection during all the phases of my life. Without the support of my family I would not be here.

Wenying Hu

CONTENTS

Page

LIST OF TABLES

LIST OF FIGURES

CHAPTER 1

INTRODUCTION

Seismic isolation is a response modification technique that reduces the effects of earthquakes on bridges and other structures. Isolation physically uncouples a bridge superstructure from the horizontal components of earthquake ground motion, leading to a substantial reduction in the force demands generated by an earthquake. Improved performance is therefore possible for little or no extra cost, and older, seismically deficient bridges may not need strengthening if treated in this manner. Uncoupling is achieved by interposing mechanical devices with very low horizontal stiffness between the superstructures (deck and girders) and substructures (columns and abutments). These devices are called seismic isolation bearings or simply isolators. Thus, when an isolated bridge is subjected to an earthquake, the deformation is concentrated in the isolators rather than the substructure elements. This greatly reduces the seismic forces and displacements transmitted from the superstructure to the substructures.

A seismic isolator possesses the three important characteristics: First, flexibility of the isolator will lengthen the period of vibration of the bridge to reduce seismic forces in the substructure. Second, energy dissipation limits displacements between the superstructure above the isolator and substructure below. Third, adequate rigidity is provided for service loads while accommodating environmental effects (Buckle et al., 2006b).

Figure 1.1 illustrates the effects of flexibility and damping of the isolator on the seismic forces. The solid and dashed curves represent the 5 percent- and 30 percent -

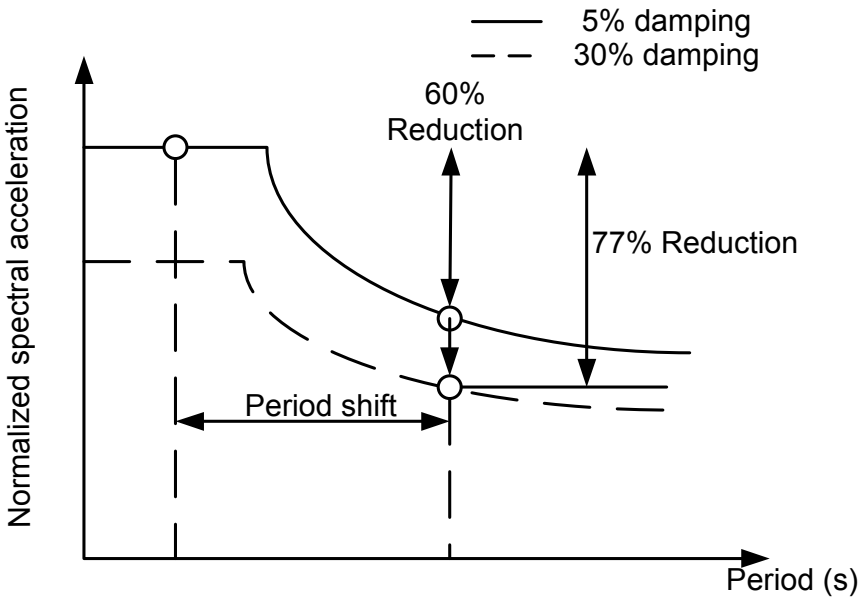

Figure 1.1 Effects of isolator on the bridge response
(Buckle et al., 2006a Figure 1-2).

damped (AASHTO, 1999) acceleration response spectra respectively, for stiff soil conditions (Soil Type Π). The increased level of damping, due to the energy dissipated by the isolation system, leads to a further reduction in the seismic forces. It is seen that period shift, or increased flexibility of the system, allows for a reduction in the spectral acceleration on the order of 60 percent, and additional reduction is possible by increasing the overall damping of the system from 5% to on the order of 30%.

Normally isolators are located at the top of all columns/abutments to separate the substructure from the deck at every location. This "fully-isolated" approach is widely accepted in the United States. Over 200 isolated bridges in the United States are currently completed or under construction. In 1988, the Eel River Bridge in Humboldt County, California, was isolated using lead-rubber bearings, very flexible elastomeric bearings with a lead core press fit in the center to increase the dissipation of energy during lateral displacements, and thus improve the performance of the bridge. This bridge experienced

accelerations of 0.55g in the 1992 Petrolia Earthquake, in which it displaced 9 inches laterally and sustained no damage (Lee, Kitane and Buckle, 2001). The Benicia-Martinez Bridge in Carquinez Straits, San Francisco Bay consists of seven 528-foot spans which provide 138 feet of vertical clearance, carrying three lanes of traffic in the southbound direction. The bridge opened in 1962 and was retrofitted in 1998 with the friction pendulum system, which consists of spherical bearings with spherical sliding interfaces (Buckle et al., 2006a).

Another approach that has been applied in a more limited context under special design circumstances is partial isolation. The Bai-Ho Bridge is completely isolated only in the longitudinal direction, while it is partially isolated in the transverse direction. Shear keys and specially designed steel rods were provided on the abutment to restrict the transverse movement of the superstructure (Shen et al., 2004). The Marga-Marga Bridge, the first bridge built in Chile with seismic bearings, is located at Viña del Mar in a high seismic risk area. The bridge consists of a single continuous 383 m superstructure supported on 36 high-damping rubber bearings that rest on two abutments and seven piers. At the abutments, isolation was provided only in the longitudinal direction. In the transverse direction, steel plate stoppers were provided to restrict motion. Transverse and longitudinal motions are allowed at piers, although an additional safety concrete stopper was provided in the transverse direction (Boroschek, Moroni and Sarrazin, 2003).

Here we refer to partial isolation as using isolators over part of the bridge. That is, isolation devices are installed at the intermediate piers, bents or columns to separate the bridge mass from the columns, while the connections of the deck to the abutments remain fixed or integral. The Utah Department of Transportation has made the strategic decision

to investigate the use of partial isolation as a routine design practice to limit the column forces. The partial isolation approach can be applied in any scenario by installing isolators at the columns that will redistribute force to the abutments from the columns and thereby limit column force demands.

The partial isolation system may be considered economical if it leads to a period shift that reduces the overall force demands on the bridge and does not increase force demands of the abutments. However, potential drawbacks to the approach include limited engagement of the isolators or overly large displacement demands at the abutments. These considerations lead to an overall question: can the partial isolation be applied as a cost-effective design approach relative to the conventional design?

The overarching objective of this research is to determine whether, or in what situations, partial isolation is effective in reducing overall forces and displacement demands on the bridge. The specific objectives of this study include: (1) develop a static design procedure for the partial isolation; (2) compare column design force and column displacement demand in conventional, fully isolated and partially isolated bridges to determine relative effectiveness of partially isolated bridges; (3) verify the accuracy and statistical reliability of the static analysis procedure for partial isolation by response history analysis; and (4) demonstrate the approach on a representative bridge in the state of Utah.

CHAPTER 2

MODEL DESCRIPTION AND PARAMETER STUDY

2.1 Simplified Bridge Models

During this research, a simplified bridge model is developed for seismic analysis to provide a generalized model of the true bridge behavior. The properties of the simplified bridge can easily be adjusted to match target spectral design criteria. In the following sections, three models are described which are conventional, fully-isolated and partially isolated bridge models

2.1.1 Conventional bridge model

The bridge superstructure is assumed to move as a rigid body under seismic loads. This assumption can be later relaxed to test the applicability of the results to more realistic bridge models. . The columns and abutments are considered as the substructure elements in these simple models. In the seismic response analysis of bridges, the substructure elements are critical to provide gravity and earthquake force transfer to the ground and ground motion input to bridge superstructure Thus, the conventional bridge model (Figure 2.1) consists of a rigid deck with weight W supported by one or more columns with total stiffness K_c and end abutments with stiffness K_a. The natural period of the bridge vibrating in its linear elastic range is calculated from the total stiffness of the bridge (K_{FB}=K_c+K_a):

$$T_n = 2\pi\sqrt{\frac{W}{K_{FB}g}} \tag{2.1}$$

Both the columns and abutments are assumed to have elastic-perfectly plastic force deformation relations (Figure 2.2) with yield force $F_{y,c}$ and $F_{y,a}$, and design displacements u_c and u_a for columns and abutments.

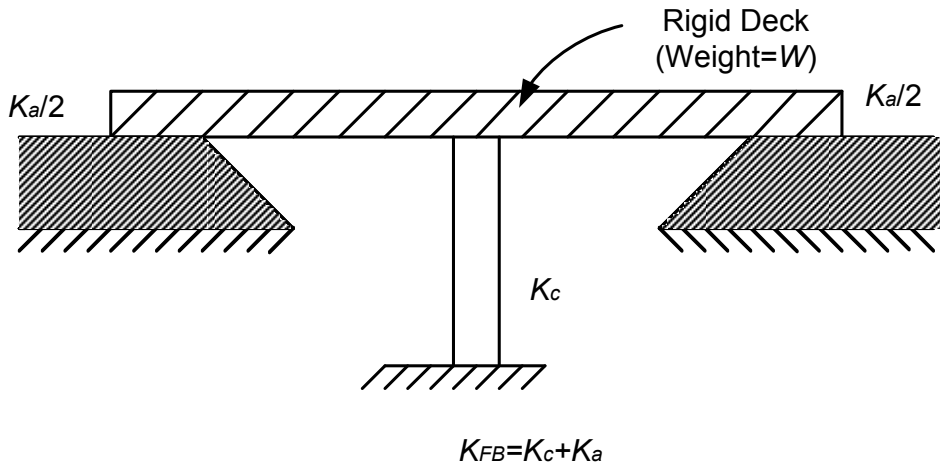

Figure 2.1 Conventional bridge model.

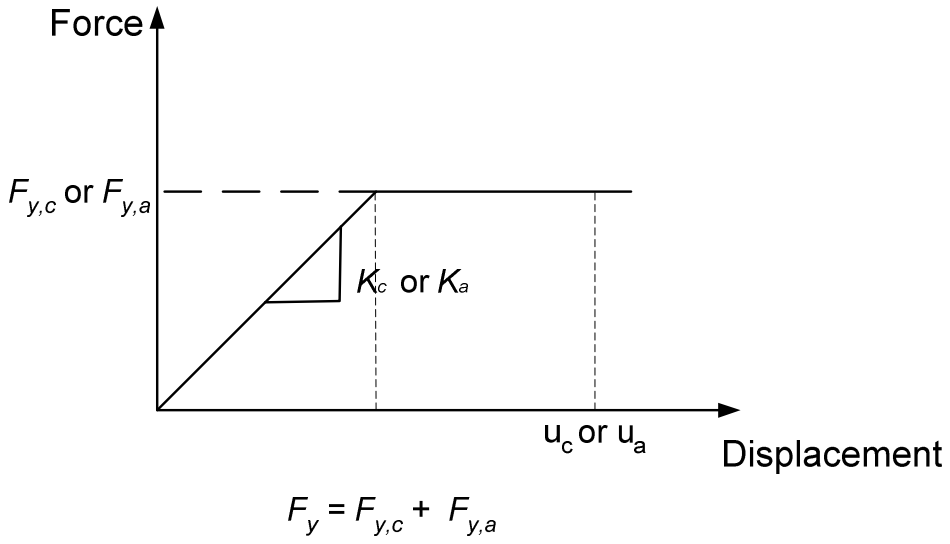

Figure 2.2 Column or abutment force/deformation relation.

2.1.2 Fully isolated bridge model

The fully isolated bridge is a conventional bridge with isolators placed on the top of every column or abutment so that the entire bridge mass is isolated or decoupled from the ground. The total stiffness K_{iso} is distributed to the isolators above the columns ($K_{iso,c}$) and abutments ($K_{iso,a}$) in proportion to their stiffness (Figure 2.3).

The period of the isolator vibrating in its linear elastic range is calculated from the total stiffness of the isolators:

$$T_{iso} = 2\pi\sqrt{\frac{W}{K_{iso}g}} \tag{2.2}$$

The force-deformation relation of the isolator is assumed to be linear with design displacement u_{iso} for the fully isolated bridge (Figure 2.4). This assumption applies to both linear devices, such as elastomeric bearings, and nonlinear devices, such as lead-rubber bearings or friction pendulum isolators, that are treated by equivalent-linear representation.

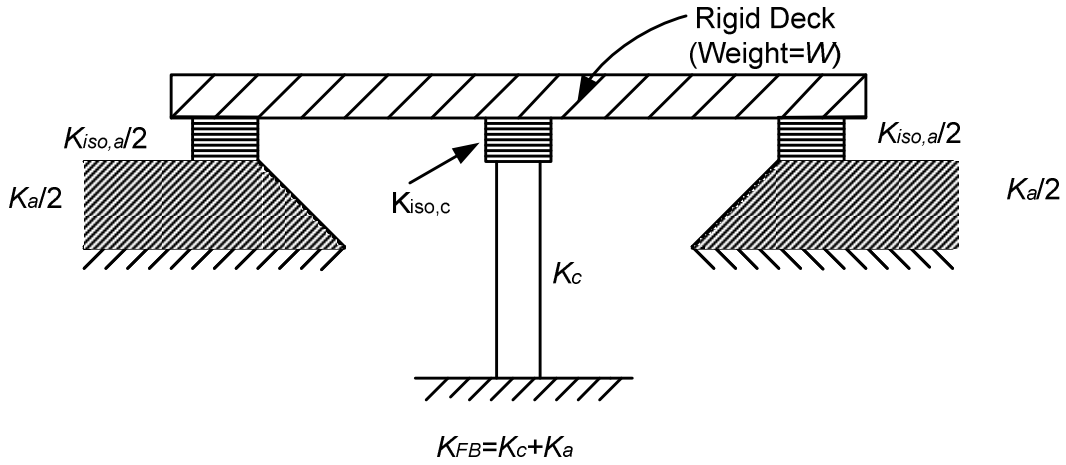

Figure 2.3 Fully isolated bridge model.

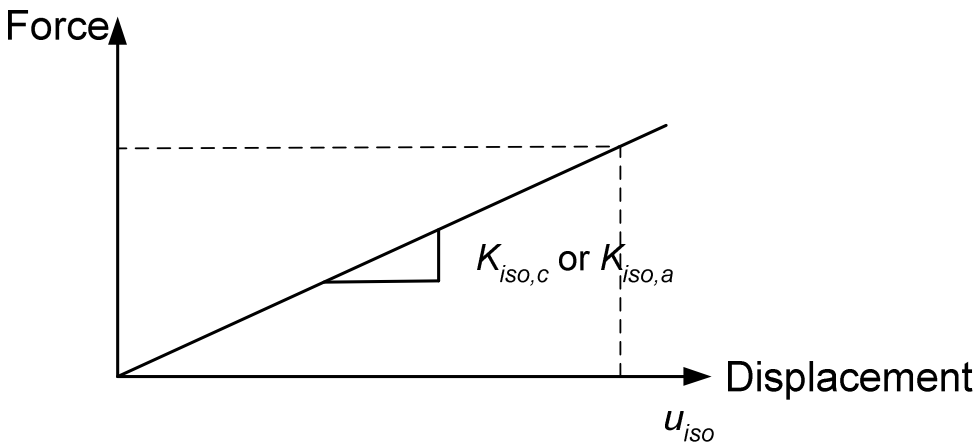

Figure 2.4 Linear isolator capacity curve.

2.1.3 Partially isolated bridge model

A partially isolated bridge is a conventional bridge with isolators placed on the top of the columns while the abutments remain fixed. Only the columns are decoupled from the ground, and in contrast to a fully isolated bridge, the stiffness of the isolator elements acts only at the columns (Figure 2.5).

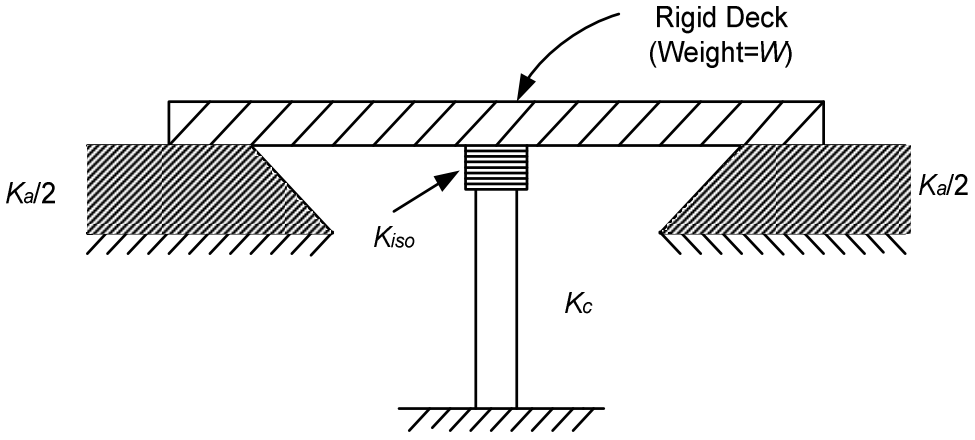

Figure 2.5 Partially isolated bridge model.

Two types of isolators are considered in this study: an equivalent linear isolator with the same properties as for the fully isolated bridge (Figure 2.4); and a nonlinear isolator with elastic-perfectly plastic force-deformation characteristics. The properties of the bilinear spring (initial stiffness k_1, yield force $F_{y,iso}$) are chosen by matching the properties of an equivalent linear system (effective stiffness K_{iso}) at the design displacement (Figure2.6). This behavior can be provided by a simple teflon slider. Sliders are often used in combination with other isolation devices, but are rarely used alone due to the absence of a restoring force (Tsopelas and Constantinou, 1997). For partial isolation, the abutment stiffness will provide a realistic limit on the overall displacement of the bridge, and sliders can be used without the risk of excessively large displacements. The yield displacement $u_{y,iso}$ of the sliding isolator is assumed to range from 0.1 cm-0.25 cm.

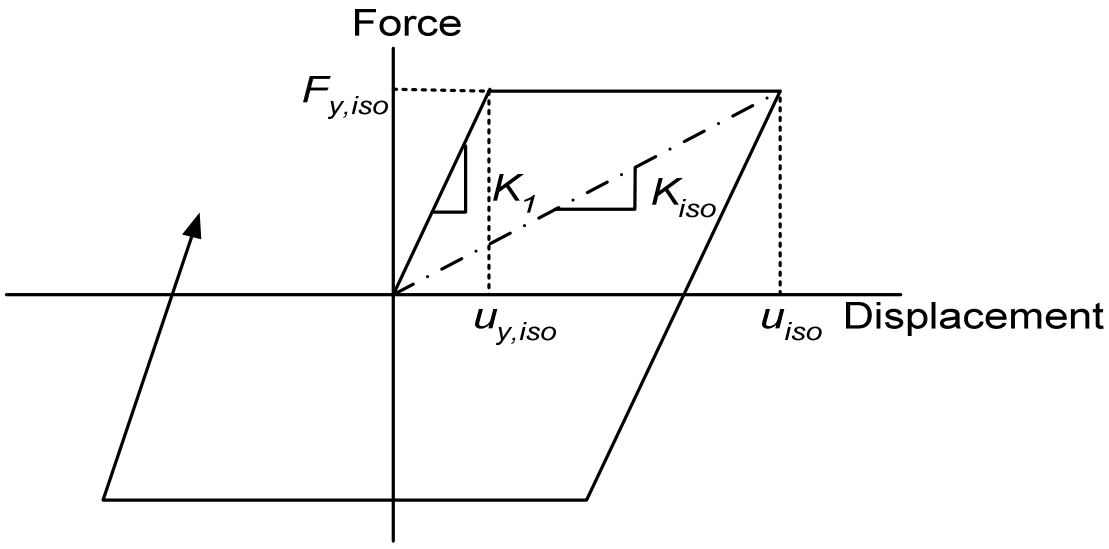

Figure 2.6 Nonlinear isolation capacity curve.

2.2 Parameter Study

A parametric study is conducted to compare the response of conventional, fully isolated and partially isolated bridges over a wide range of bridge parameters described in the general bridge model of the previous section. Independent parameters are hereby identified and varied over the ranges indicated.

The natural period T_n of a conventional bridge before isolation is applied (Equation (2.1)) is varied from 0 to 1 with distinct values of [T_n = 0.1,0.2,0.3,0.4,0.5,0.6,0.7,0.8,0.9,1.0]. This range includes UDOT's typical short span highway bridges that are likely candidates for partial isolation. The isolation period T_{iso} takes on values of 1, 2, 2.5, 3, 3.5, 4 sec, where conventionally the longer isolation period leads to a greater isolation effect. The damping ratios of the linear isolator ζ_{iso} are chosen as 5%, 10%, 20%, and 30%, while the damping ratio of an elastic-perfectly plastic isolator will be shown to be constant.

Two parameters are defined that quantify the distribution of stiffness and strength to the columns and the abutments:

$$\alpha_k = \frac{K_c}{K_c + K_a} \tag{2.3}$$

$$\alpha_F = \frac{F_{y,c}}{F_{y,c} + F_{y,a}} \tag{2.4}$$

α_k is the column stiffness ratio, or ratio of the column stiffness to the total bridge stiffness, and α_F is the column strength ratio, or ratio of the column strength relative to the total bridge strength. The value of α_k is assumed to vary essentially from 0 to 1, taking on distinct values [0.1, 0.2, 0.3, 0.4, 0.5, 0.6, 0.7, 0.8, 0.9], and α_F is assumed to

equal $\alpha_{k..}$ Table 2.1 lists the parameters that apply to each bridge model (conventional, fully isolated, and partially isolated).

Table 2.1 List of parameters for each bridge model

Conventional bridge	**Fully isolated bridge**	**Partial isolated bridge**
α_k	α_k	α_k
α_F	α_F	α_F
ζ	ζ	ζ
-	ζ_{iso}	ζ_{iso}
-	ζ_{eff}	ζ_{eff}
W	W	W
T_n	T_{iso}	T_{iso}
B	B	B
-	B_{eff}	B_{eff}
K_c	K_c	K_c
K_a	K_a	K_a
-	K_{iso}	K_{iso}
-	$K_{iso,c}$	-
-	$K_{iso,a}$	-
$F_{y,c}$	$F_{y,c}$	$F_{y,c}$
$F_{y,a}$	$F_{y,a}$	$F_{y,a}$
u_c	u_c	u_c
u_a	u_a	u_a
-	u_{iso}	u_{iso}
F	F	F
F_y	F_y	F_y
K_{FB}	K_{FB}	K_{FB}
D	D	D
-	K_{eff}	K_{eff}

CHAPTER 3

STATIC EVALUATION PROCEDURE

In this chapter, static evaluation procedures for linear and nonlinear partially isolated bridge are developed to be consistent with evaluation procedures for conventional and fully isolated bridge models.

3.1 Design Response Spectrum

3.1.1 Response spectrum for conventional bridge

For static evaluation, a design spectrum is calculated assuming a bridge located in Salt Lake City, Utah (zip code: 84040), on soil site class D. The spectral acceleration coefficients, based on a 2500 year return period motion (or 2% probability of exceedance in 50 years) are given in the table below (Table 3.1).

For the conventional bridge, the seismic base shear, F, in each direction is determined according to (AASHTO, 2002):

$$F = C_s W \tag{3.1}$$

$$C_s = \frac{1.2AS}{T_n^{\frac{2}{3}}} \leq 2.5A \tag{3.2}$$

where C_s is the seismic response coefficient, A is the peak spectral response acceleration parameter ($A = 0.4FvSs$), and S is the site coefficient. For the Salt Lake City location, A=0.549 and S= 1.5 for Site class Π.

Table 3.1 Spectral acceleration coefficient for the special site

Ground motions(T_R)	*Ss* (g)	*Fv*	*S1* (g)	*Fa*
2500years	1.364	1.0	0.569	1.5

3.1.2 Response spectrum for isolated bridge

According to current bridge codes, the design spectrum for isolated bridges differs from that of conventional bridges. The design spectrum is specified in terms of a design displacement D rather than spectral acceleration, which is a function of the effective period T_{eff} and damping ratio ζ_{iso} of the bridge. According to AASHTO (1999):

$$D = 10\, A\, S_i\, T_{eff} / B_{iso} \quad \text{(inches)} \tag{3.3}$$

where

$$T_{eff} = 2\pi\sqrt{W / gK_{eff}} \tag{3.4}$$

B_{iso} is a damping factor that depends on the damping ratio ζ_{iso}, A is the acceleration coefficient for the site, and S_i is the site coefficient for isolated structure. In this study, the acceleration coefficient A (which represents peak ground acceleration) is replaced by the 1.0 second period spectral acceleration coefficient S_1 (Buckle et al., 2006a).

The total lateral force in the system can be estimated from the displacement D according to:

$$F = K_{eff} D \tag{3.5}$$

For this location assuming site class III, the soil coefficient Si = 2.0 and S_1= 0.569. Note that this value is larger than the soil coefficient for a comparable conventional bridge and accounts for long period spectral amplification in soft soils.

The design spectra for conventional and isolated bridges for the site are compared in Figure 3.1.

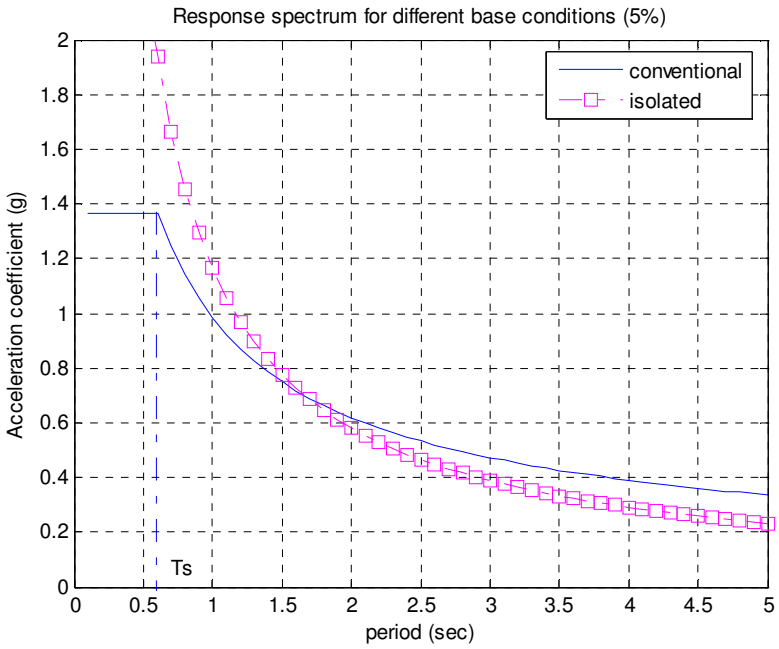

Figure 3.1 Response spectrums for the bridges with different bases.

The spectrum for conventional bridges exceeds that for isolated bridges in the long period range because T is taken to the power of 2/3. The spectrum of Figure 3.1 is for 5% damping and spectral accelerations for other values of damping are found by dividing by the appropriate damping factor.

3.2 Static Design and Analysis Equations

3.2.1 Conventional bridge

The response modification factor (R) is used to calculate the design force from the elastic force demand. The response modification factor contains two components (Constantinou and Quarshie, 1998):

$$R = R_{\mu} \cdot R_{o} \tag{3.6}$$

where R_μ is ductility-based portion of the factor and R_O is overstrength factor. The ductility-based portion R_μ is the result of inelastic action in the structural system. The overstrength factor R_O is the result of reverse strength that exists between the design force and actual yield force of the system (Constantinou and Quarshie, 1998). Since the capacity of the columns or abutments to resist lateral loads is idealized as elastic-perfectly plastic for the conventional bridge, only R_μ is considered. Normally R values range from 2 to 5 for substructures (columns and abutments) (AASHTO, 1999), and a typical value of R_O is 1 to 1.67. Thus, R_μ=3 is assumed for this study, consistent with R=5 and R_O=1.67.

Based on the known weight W, the assumed natural period of the bridge T_n, the 5% damped design spectrum S_a, and an assumed R-factor, the stiffness K_{FB} and design base shear F (Equations (3.1) and (3.2)) can be estimated.

$$K_{FB}= \frac{W}{g}\left(\frac{2\pi}{T_n}\right)^2 \tag{3.7}$$

Assuming a column strength ratio α_k, the column stiffness K_c and the abutment stiffness K_a are calculated from the total stiffness K_{FB} according to:

$$K_c= K_{FB}\,\alpha_k \tag{3.8}$$

$$K_a = K_{FB}\,(1-\alpha_k) \tag{3.9}$$

The design base shear of the whole bridge F_y is calculated from the elastic base shear F and force reduction R.

$$F_y = \frac{F}{R} \tag{3.10}$$

Assuming a column strength ratio α_F, the column yield force $F_{y,c}$ and the abutment yield force $F_{y,a}$ are calculated from the total yield force F_y according to:

$$F_{y,c} = F_y \alpha_F \tag{3.11}$$

$$F_{y,a} = F_y (1-\alpha_F) \tag{3.12}$$

The displacement demand D is determined from the design spectrum, but an adjustment may be required to account for the overall nonlinear response of the bridge. A transition period T^* is defined:

$$T^* = 1.25 T_s \tag{3.13}$$

where T_s is the end of the flat part of the response spectrum, valued at 0.6261 second for the conventional bridge design spectrum (Figure 3.1). If $T_n > T^*$, the equal displacement rule applies and the actual displacement is assumed to be the same as the linear displacement.

$$D = \frac{F}{K_{FB}} = \frac{C_S T_n^2}{4\pi^2 g} \tag{3.14}$$

If $T_n < T^*$, an increase in D is calculated according to the following equations (Friedland, Mayes, and Bruneau, 2001):

$$D = [(1-1/R)\, T^*/Tn + 1/R] \frac{F}{K_{FB}} = \frac{C_S T_n^2}{4\pi^2 g} \quad [(1-1/R)\, T^*/Tn + 1/R] \tag{3.15}$$

The column and abutment displacements of the conventional bridge are identical to the total bridge displacement.

$$u_c = u_a = D \tag{3.16}$$

3.2.2 Fully isolated bridge

By simple analysis, Constantinou and Quarshie (1998) showed that the effectiveness of the isolation system diminishes and larger displacement demands are imposed on the substructure when the inelastic action commences in the substructure for the isolated bridge. Therefore, the allowable *R*-factors were reduced to the range of 1.5 to 2.5 (AASHTO, 1999), which implies that R_μ is between 1 and 1.5. In this study, R_μ is assumed to be 1.

Since both the bridge and isolation system are assumed to remain elastic, the effective stiffness is computed as the stiffness of the bridge and the isolation system acting in series.

$$K_{eff} = \frac{K_{FB} K_{\text{iso}}}{K_{FB} + \text{K}_{\text{iso}}} \tag{3.17}$$

The stiffness of the substructure (K_{FB}) is calculated from Equation (3.7) and K_{iso} is computed from an assumed isolation period according to:

$$K_{iso} = \frac{W}{g}\left(\frac{2\pi}{T_{iso}}\right)^2 \tag{3.18}$$

The isolator stiffness is distributed to the columns and abutments in proportion to their stiffness:

$$K_{iso,\,c} = K_{iso}\,\alpha_k \tag{3.19}$$

$$K_{iso,a} = K_{iso}\,(1-\alpha_k) \tag{3.20}$$

The displacement demand *D*, elastic strength F and yield force F_y can be calculated from Equations (3.3-3.5) and Equation (3.10), where the effective damping

ratio of the bridge is assumed to equal the damping ratio of the isolation system. The yield force F_y is simply equal to the elastic strength F, and is distributed to the columns and abutments in proportion to their strengths (Equations (3.11) and (3.12)). Since the isolation system and bridge substructure act in series, the displacement demand D is distributed to the isolators and substructures in proportion to their flexibilities.

$$u_{iso} = \frac{F}{K_{iso}} \tag{3.21}$$

$$u_c = u_a = \frac{F}{K_{FB}} \tag{3.22}$$

3.2.3 Partially isolated bridge.

As described earlier, two different types of isolation systems are considered for partially isolated bridges. The isolation systems lead to very different dynamic behaviors and thus use different analysis procedures.

3.2.3.1 Linear isolation system. If the bridge is partially isolated with linear devices, the performance of the columns will degrade once their elastic limit has been reached and larger displacement demands will be imposed on the substructure. Therefore, similar to the philosophy for fully isolated bridges, R_μ=1 is selected to limit inelastic demands to the columns, and the bridge is analyzed using the design spectrum for the isolated bridge (Equation (3.3)), with the exception that the spectral acceleration should not exceed the constant short period acceleration of the spectrum for the conventional bridge if the period shift is not large enough to force the bridge into the constant velocity region of the spectrum.

The total stiffness (K_{FB}) and its distribution to the columns and abutments (K_c, K_a) is determined as for the conventional bridge (Equations (3.7) - (3.9)) assuming a natural period T_n. The stiffness of the isolator on the top of the columns is based on the isolation period (T_{iso}) and the fraction of total bridge stiffness carried by the columns (α_k):

$$K_{iso} = \frac{W}{g}\left(\frac{2\pi}{T_{iso}}\right)^2 \alpha_k \tag{3.23}$$

The effective stiffness is calculated by adding the composite stiffness of the column\isolator unit and the abutment stiffness K_a.

$$K_{eff} = \frac{K_c K_{iso}}{K_c + K_{iso}} + K_a \tag{3.24}$$

T_{eff} is calculated from K_{eff} (Equation (3.4)).

To apply the static procedure, an appropriate damping ratio for the entire bridge must be selected. Because full isolation is not observed, it is unconservative to assume that the damping ratio equals the effective damping of the isolation system. Similar to fully isolated bridge, the contribution of damping from the columns and abutments is ignored. The effective damping ratio for the whole bridge is decreased by the column stiffness ratio, which represents the fraction of the bridge to which the isolator stiffness is applied, and adjusted for the modified effective period relative to the isolation period.

$$\xi_{eff} = \xi_{iso}\alpha_k\left(\frac{T_{eff}}{T_{iso}}\right) \tag{3.25}$$

However, the effective damping ratio is assumed not to fall below 5%, since the damping ratio in the conventional bridge must be a lower bound to the damping ratio of the bridge with any type of protective devices. The damping factor B_{iso} is determined based on ξ_{eff}

Table 3.2 of Buckle et al., 2006a) and the displacement demand *D* from Equation(3.2). The force demand *F* is computed assuming linear elastic response. (Equation (3.5))

Since the columns remain elastic under the design motion, the total displacement demand *D* is distributed to the isolators and columns in proportion to their stiffness:

$$u_{iso} = \frac{D}{1+\frac{K_{iso}}{K_c}} \tag{3.26}$$

$$u_c = D - u_{iso} \tag{3.27}$$

The abutments see the entire displacement:

$$u_a = D \tag{3.28}$$

The yield force of columns and abutments ($F_{y,c}$, $F_{y,a}$) are calculated by the same procedure as for the fully isolated bridge (Equations(3.10) - (3.12)).

3.2.3.2 Nonlinear isolation system. The main benefit of using isolation devices with elastic-perfectly plastic behavior, such as sliding isolators, is that the isolators can be designed to yield first, thus keeping the columns elastic. As a result, it is not necessary to design the entire bridge to remain elastic to see improved column forces, and a bridge force reduction factor R_μ=3 is imposed, as in the conventional bridge.

The yield force of the column is assumed to be 10% greater than the yield force of the isolator, as a factor of safety against yielding.

$$F_{y,c}=1.1F_{y,iso} \tag{3.29}$$

The parameters $K_{iso,}$ $K_{a,}$ $K_{c,,}$ K_{eff} ,T_{eff} are calculated according to the procedure for the partially isolated bridge with linear isolator (Equations (3.23)-(3.24) and (3.8)-(3.9)). Because the bridge is not isolated in a conventional sense, the conventional AASHTO

spectrum is used (Equations (3.1) and (3.2)) with T_{eff} instead of T_n and the design base shear F_y is calculated using the procedure for conventional bridge (Equation (3.10))

Since the goal is to reduce demands on the columns compared to a conventional bridge, the abutments are assumed to have the same yield force as in the conventional bridge, and all reductions in force demand that may result from partial isolation are passed to the columns:

$$F_{y,a} = F_{y,a(con)} \tag{3.30}$$

$$F_{y,iso} = F_y - F_{y,a} \tag{3.31}$$

The total bridge displacement is calculated by the same procedure as for the conventional bridge, which assumes displacement amplification in the short period range (Equations (3.14) and (3.15)). Since the columns do not yield when the isolators yield:

$$u_c = \frac{F_{y,iso}}{K_c} \tag{3.32}$$

$$u_{iso} = D - u_c \tag{3.33}$$

The abutment displacement equals the total bridge displacement.

$$u_a = D \tag{3.34}$$

The spectral displacement D is a function of the bridge damping ratio, which is calculated from the effective damping in the isolator. The effective damping ratio of the elastic-perfectly plastic isolator is calculated by equating the energy dissipation of the hysteretic loop with the energy dissipated in viscous damping (Figure 3.2) (Chopra, 2000).

The damping ratio of the elastic-perfectly plastic isolator is given by:

$$\varsigma = \frac{1}{4\pi}\frac{W_D}{E_s} = \frac{1}{4\pi}\frac{4F_{y,iso}u_{iso}}{\frac{1}{2}F_{y,iso}u_{iso}} = \frac{2}{\pi} = 0.63 \tag{3.35}$$

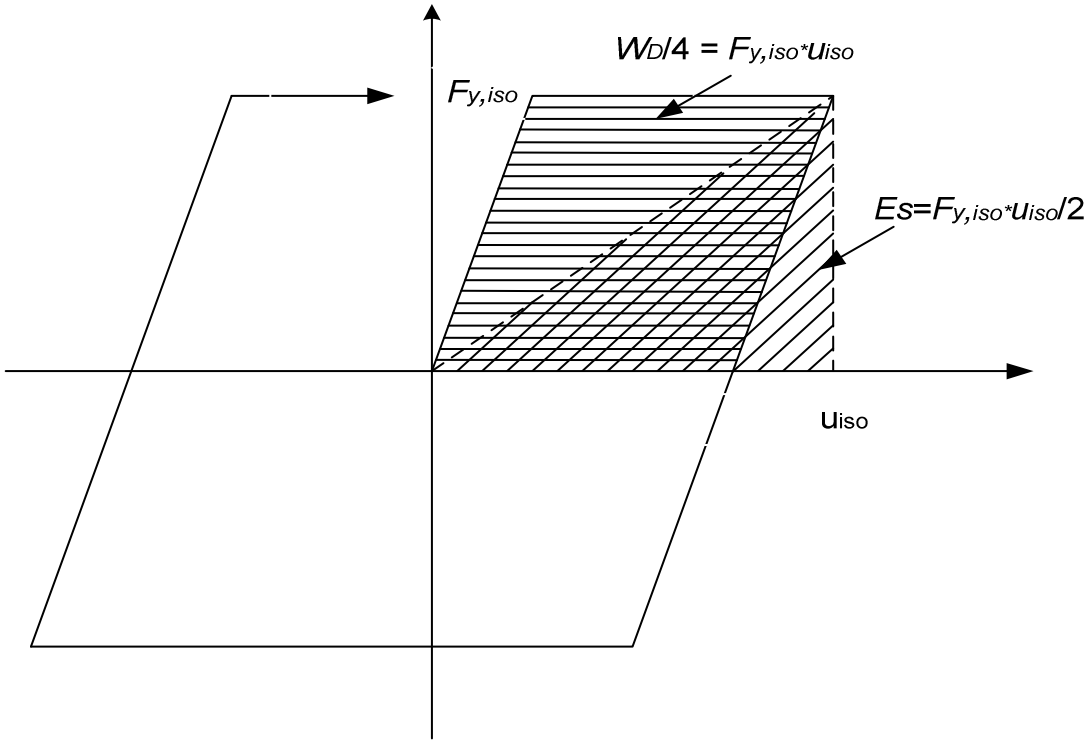

Figure 3.2 Definition of energy dissipation W_D and strain energy Es for nonlinear isolator.

where E_s is the strain energy and W_D is the energy dissipated in one hysteresis cycle. The damping ratio of isolation devices is calculated to be 63% and independent of displacement when the devices are elastic-perfectly plastic. A similar procedure is used to estimate the effective damping ratio of the whole bridge, whereby strain energy E_s of the whole bridge replaces that of the elastoplastic device.

$$E_{s,\,bridge} = Fu_a / 2 \tag{3.36}$$

$$\xi_{eff} = \frac{2}{\pi}\left(\frac{F_{y,iso}}{F}\right)\left(\frac{u_{iso}}{u_a}\right) \tag{3.37}$$

The linear elastic strain energy is used, which will lead to a conservative estimate of the damping ratio. Again, ξ_{eff} is constrained to be at least 5% such that it does not fall below the damping ratio in a conventional bridge.

Note that the procedure to calculate ξ_{eff} is iterative because the forces and displacements depend on ξ_{eff}. An initial damping ratio of 5% is assumed and the procedure is terminated after one iteration. Table 3.2 summarizes the equations used to evaluate the bridges with different base conditions.

Increased energy dissipation is an important part of the seismic isolation concept. Figure 3.3(a), (b), (c) and (d) show the effective damping ratios computed from Equations (3.25) and (3.37) as a function of α_k and T_n for linear and nonlinear partial isolation. From these figures, the effective damping ratio is observed to be 5% when α_k is very small. The effective damping ratio of linear partial isolation increases with increasing α_k and increasing T_n but decreases when T_{iso} increases. The effective damping ratio of nonlinear partial isolation increases when α_k increases and decreases when T_n increases, expect in short period range which is the constant acceleration part of the spectrum. However, the isolation period does not much influence the effective damping ratio for nonlinear partial isolation compared with linear partial isolation. The partial isolation is expected to be most effective when the effective damping ratio is substantially larger than 5%.

Table 3.2 Summary of static procedure

Conventional	Full Isolation	Partial Isolation	
		Linear	nonlinear
$R=3$	$R=1$	$R=1$	$R=3$
$K_{FB}= \frac{W}{g}\left(\frac{2\pi}{T_n}\right)^2$	$K_{FB}= \frac{W}{g}\left(\frac{2\pi}{T_n}\right)^2$	$K_{FB}= \frac{W}{g}\left(\frac{2\pi}{T_n}\right)^2$	$K_{FB}= \frac{W}{g}\left(\frac{2\pi}{T_n}\right)^2$
$K_c= K_{FB}\ \alpha_k$	$K_c= K_{FB}\ \alpha_k$	$K_c= K_{FB}\ \alpha_k$	$K_c= K_{FB} \times \alpha_k$
$K_a= K_{FB}\ (1-\alpha_k)$	$K_a= K_{FB}\ (1-\alpha_k)$	$K_a= K_{FB}\ (1-\alpha_k)$	$K_a= K_{FB}\ (1-\alpha_k)$
-	$K_{iso}= \frac{W}{g}\left(\frac{2\pi}{T_{iso}}\right)^2$	$K_{iso} = \frac{W}{g}\left(\frac{2\pi}{T_{iso}}\right)^2 \alpha_k$	$K_{iso} = \frac{W}{g}\left(\frac{2\pi}{T_{iso}}\right)^2 \alpha_k$
-	$\xi_{eff}= \xi_{iso}$	$\xi_{eff}= \xi_{iso}\alpha_k\left(\frac{T_{eff}}{T_{iso}}\right)$	$\xi_{eff}= \frac{2}{\pi}\left(\frac{F_{y,iso}}{F}\right)\left(\frac{u_{iso}}{u_a}\right)$
-	$K_{eff} = \frac{K_{FB}K_{iso}}{K_{FB}+K_{iso}}$	$K_{eff}= \frac{K_c K_{iso}}{K_c + K_{iso}} + K_a$	$K_{eff}= \frac{K_c K_{iso}}{K_c + K_{iso}} + K_a$
-	$T_{eff} = 2\pi\sqrt{\frac{W}{K_{eff}\, g}}$	$T_{eff} = 2\pi\sqrt{\frac{W}{K_{eff}\, g}}$	$T_{eff} = 2\pi\sqrt{\frac{W}{K_{eff}\, g}}$
$D = \frac{C_S T_n^2}{4\pi^2 g}$ ($Tn > T^*$) or $\frac{C_S T_n^2}{4\pi^2 g}$ * [(1-1/R) T*/T+1/R] ($Tn < T^*$)	$D=10\ Si\ S1\ T_{eff}/B_{iso}$	$D=10\ Si\ S1\ T_{eff}/B_{eff}$	$D = \frac{C_S T_n^2}{4\pi^2 g}$ ($Tn > T^*$) or $\frac{C_S T_n^2}{4\pi^2 g}$ * [(1-1/R) T*/T+1/R] ($Tn < T^*$)
$Cs = \frac{1.2AS}{T_n^{2/3}} \le 2.5A$, $F = CsW$	$F= K_{eff}D$	$F= K_{eff}D$	$Cs = \frac{1.2AS}{T_{eff}^{2/3}} \le 2.5A$, $F = CsW$
$F_y = \frac{F}{R}$	$F_y = \frac{F}{R}$	$F_y = \frac{F}{R}$	$F_y = \frac{F}{R}$
$F_{y,a} = F_y\ (1-\alpha_F)$	$F_{y,a} = F_y\ (1-\alpha_F)$	$F_{y,a} = F_y\ (1-\alpha_F)$	$F_{y,a} =F_{y,a(con)}$
-	-	-	$F_{y,iso}=F_y-F_{y,a}$
$F_{y,c} = F_y\alpha_F$	$F_{y,c} = F_y\alpha_F$	$F_{y,c} = F_y\alpha_F$	$F_{y,c}=1.1F_{y,iso}$
-	$u_{iso} = \frac{F}{K_{iso}}$	$u_{iso} = \frac{D}{1+\frac{K_{iso}}{K_c}}$	$u_{iso}= D- u_c$
$u_c =D$	$u_c = F/ K_{FB}$	$u_c = D- u_{iso}$	$u_c =F_{y,iso}/K_c$
$u_a = D$	$u_a=F/ K_{FB}$	$u_a = D$	$u_a = D$

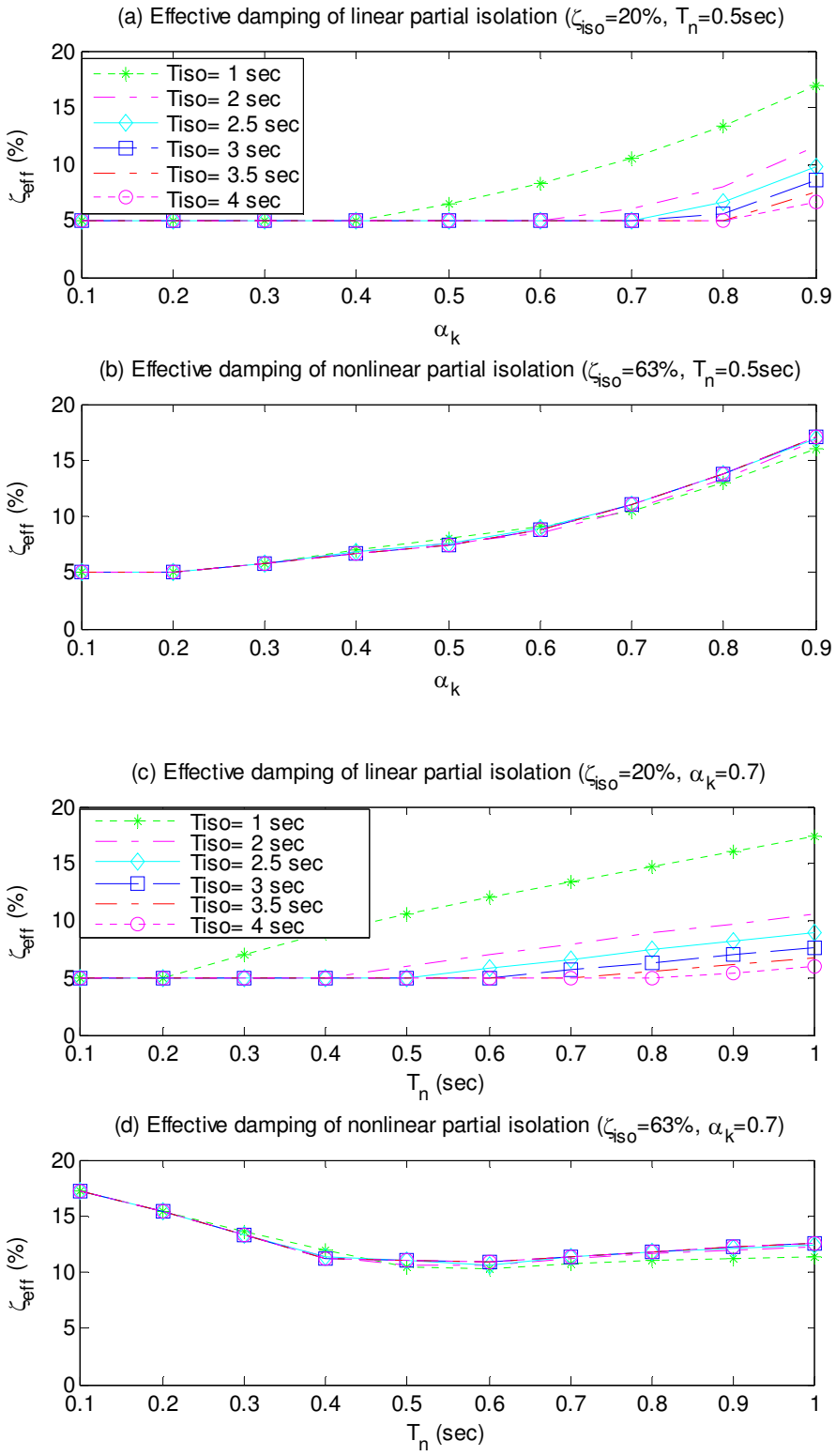

Figure 3.3(a) - (d) Comparison of ζ_{eff} for linear and nonlinear partial isolations.

CHAPTER 4

EVALUATION OF PARTIAL ISOLATION BASED ON STATIC ANALYSIS

In this section, the linear and nonlinear partial isolation approaches are evaluated in their ability to reduce column displacement and force demands relative to a conventional bridge and a fully isolated bridge for a wide range of bridge parameters. Abutment displacement demands are expected to increase with partial isolation, but must be limited to reasonable values. Throughout this chapter, the demands in the fully and partially isolated bridge, computed from the static equations developed in Chapter 3, are presented in normalized from relative to the demands in a conventional bridge. However, to provide some perspective, Figure 4.1(a)-(d) show the absolute values of the displacement and force demands of the column and abutment, varying with the substructure period (T_n) when α_k=0.7 and T_{iso}=3 sec for different bridge models.

Figures 4.2 and 4.3 illustrate the column displacement ratios of different. isolation approaches relative to conventional bridge ($u_c / u_{c,con}$), considering variation of α_k (Figure 4.2) and T_n (Figure 4.3). The column displacement trends as a function of α_k are similar for full isolation (Figure 4.2(a)) and linear partial isolation (Figure 4.2(b)): the column displacement ratio is essentially independent of the column stiffness distribution α_k and decreases with increasing isolation period T_{iso}, but converges to a lower bound as the isolation period becomes very large. The column displacement reduces a lot compared to a conventional bridge.

For nonlinear partial isolation the column displacement demand ratio ($u_c / u_{c,con}$) (Figure 4.2(c)), decreases sharply with increasing α_k and is not very sensitive to the isolation period. Increasing column participation (α_k) causes the effective period to

increase for nonlinear partial isolation, which reduces the yield force and hence the column displacements since the columns remain elastic. Nonlinear partial isolation is not effective to improve the performance of bridges with very low column stiffness. Thus in this study, small column participation (α_k< 0.2) and low natural periods (T_n<0.2) are not discussed.

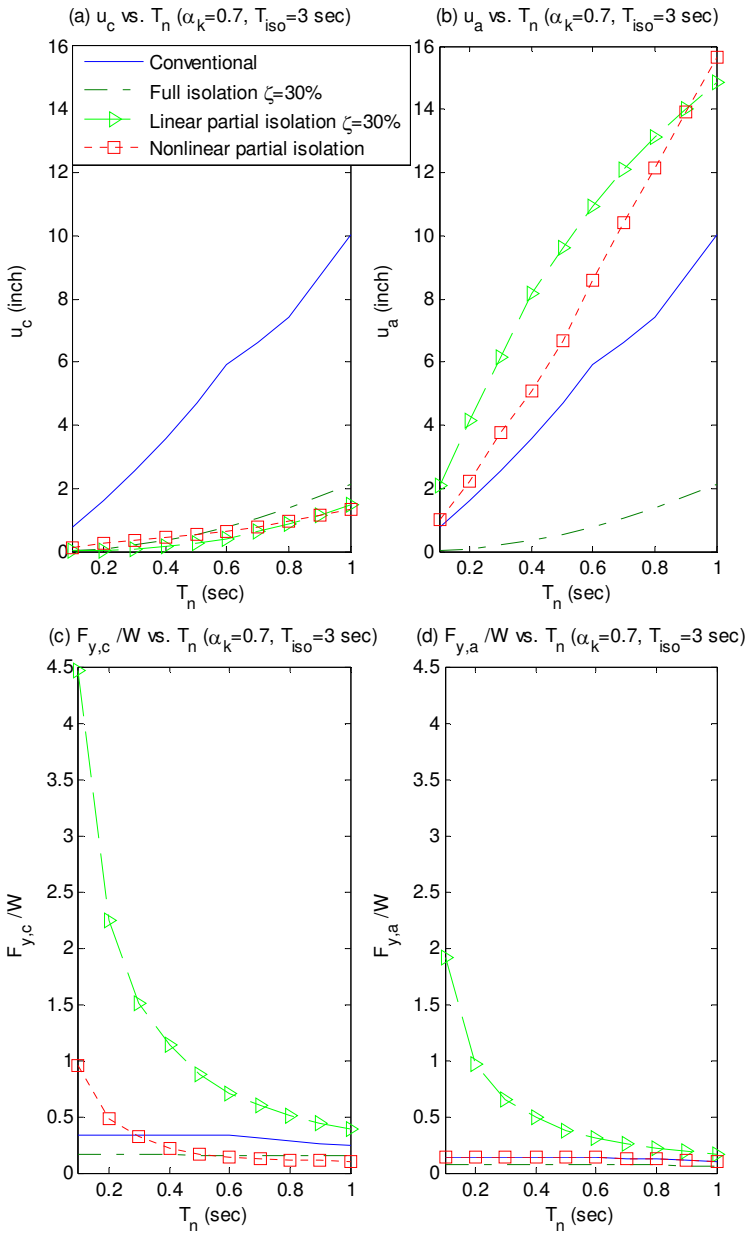

Figure 4.1(a) - (d) Comparison of force and displacement demands for different bridges.

For a specified α_k =0.7 and T_{iso}=3 sec, increasing the isolation damping ratio ζ_{iso} further lowers the column displacements of a fully isolated bridge (Figure 4.3(a)), but has little influence on the column displacements for linear partial isolation (Figure 4.3(b)). Increasing T_n causes the column displacement ratio to increase for both full and linear partial isolation but still remain well less than 1.

For nonlinear partial isolation (Figure 4.3(c)), the column displacement ratio decreases a little bit in the region T_n <0.4, then increases beyond T_n = 0.6 sec. In the low period region (T< T*), the effective period of nonlinear partial isolation is larger than the natural period of the conventional bridge, so the column displacement demands for nonlinear partial isolation increase more slowly than for a conventional bridge.

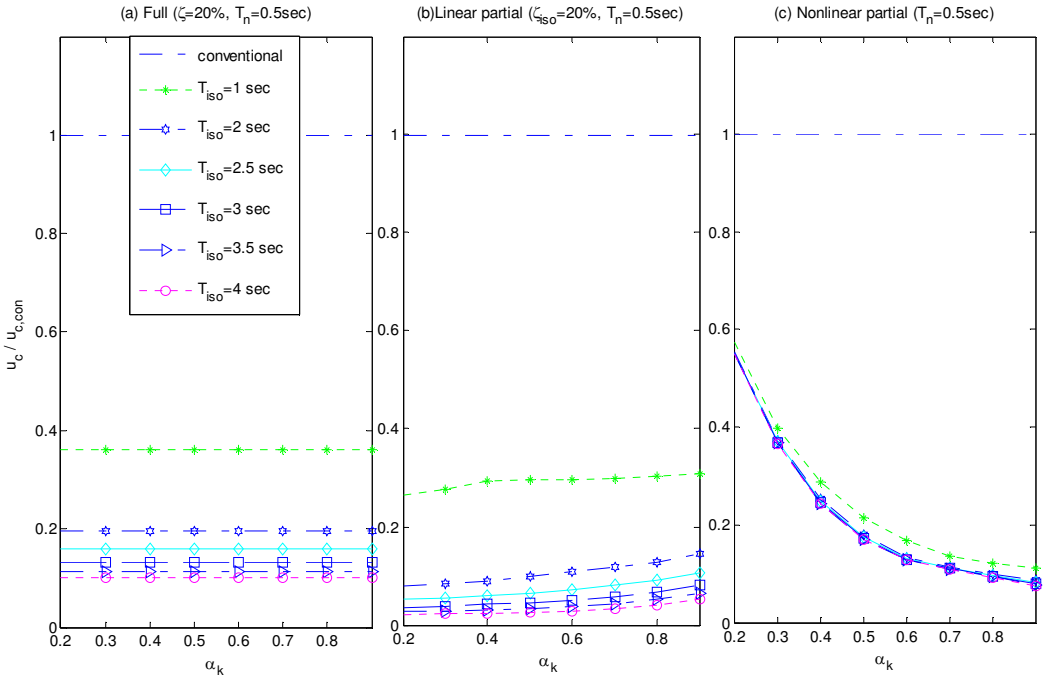

Figure 4.2 (a) - (c) u_c / $u_{c,con}$ vs. α_k for different isolation systems.

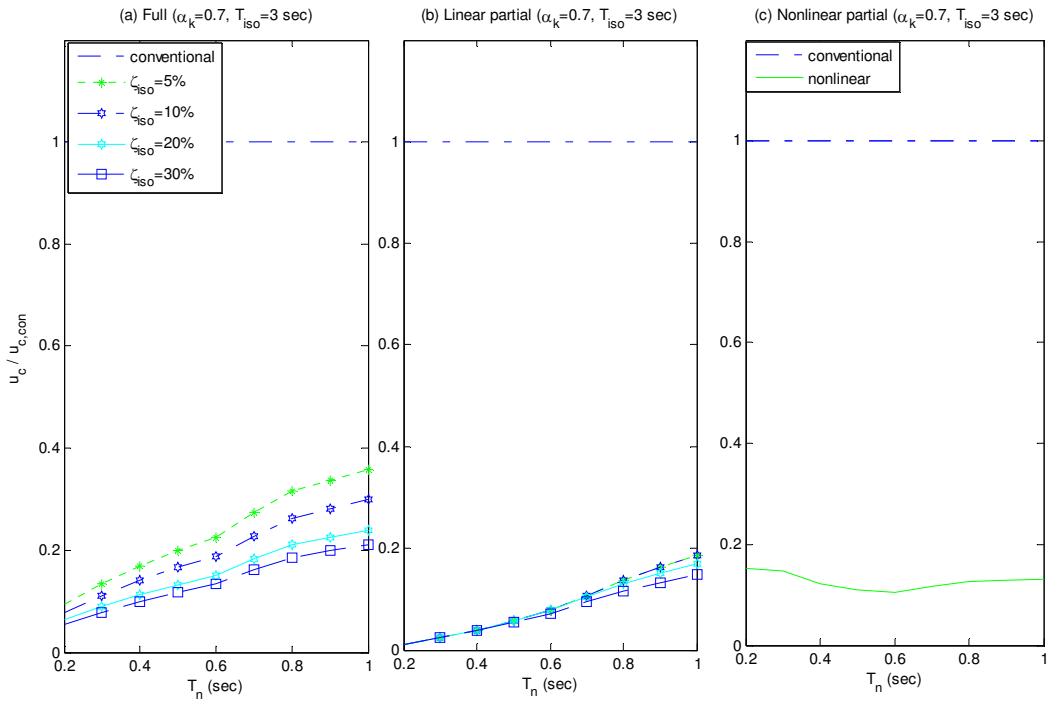

Figure 4.3 (a) - (c) $u_c / u_{c,con}$ vs. T_n for different isolation systems.

Overall, the column displacement demand u_c is very small compared with a conventional bridge for both partial isolation approaches assuming the columns have substantial stiffness participation (α_k =0.7). For linear partial isolation, the isolation and substructure periods determine the reduction in column displacement, while for nonlinear partial isolation, the column stiffness ratio (α_k) determines the reduction of column displacement. In general, partial isolation is as effective as full isolation in reducing column displacement demands.

Figures 4.4 and 4.5 present the column yield force relative to conventional bridge ($F_{y,c} / F_{y,c(con)}$) for the various isolation approaches. While full isolation generally reduces the column force demand below that of a conventional bridge unless the period shift is insufficient (Figure 4.4(a)), linear partial isolation is ineffective in reducing the force

demand in the columns below that of a conventional bridge over any range of parameters (Figure 4.4(b), 4.5(b)). The column yield force ratio decreases with increasing isolation period and with increasing effective damping ratio, but the column yield force ratio is never less than 1. The main reason is that the period shift and increase in damping of partial isolation is modest compared to full isolation. Thus, the decrease in force demand due to modification of system properties can never overcome the substantial increase associated with decreasing R from 3 to 1, as assumed for linear partial isolation.

For nonlinear partial isolation the force demand in the columns are reduced effectively when $\alpha_k > 0.4$ (Figure 4.4(c)), and when $T_n > 0.3$sec for T_{iso}= 3sec (Figure 4.5(c)). Nonlinear partial isolation is more effective in reducing column displacements since it uses the same force reduction factor as a conventional bridge and benefits positively from slight changes in stiffness and damping.

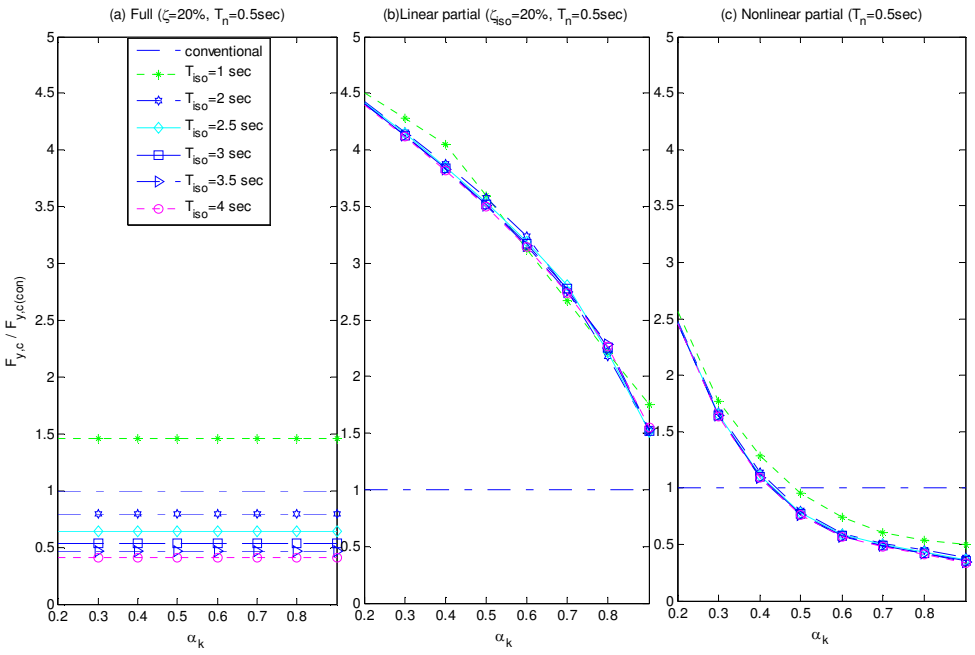

Figure 4.4 (a) - (c) $F_{y,c} / F_{y,c(con)}$ vs. α_k for different isolation systems.

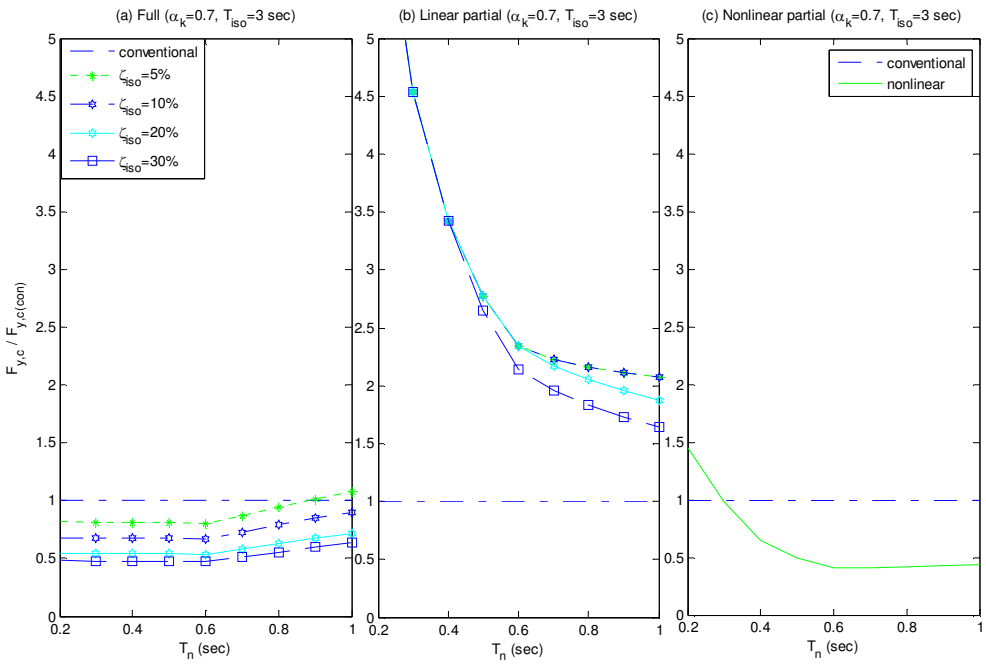

Figure 4.5 (a) - (c) $F_{y,c} / F_{y,c(con)}$ vs. T_n for different isolation systems.

Figure 4.6 (a)-(c) and Figure 4.7 (a)-(c) illustrate the abutment displacement demands of fully and partially isolated bridges relative to the conventional bridge (u_a/ $u_{a,con}$) for various parameters. For the fully isolated bridge, the abutment displacement is identical to the column displacement, and decreases substantially compared to a conventional bridge (Figure 4.6(a), 4.7(a)). However, the abutment displacement u_a in a partially isolated bridge always exceeds that of a conventional bridge, for all values of α_k (Figure 4.6 (b), (c)) and T_n (Figure 4.7 (b), (c)). This behavior is expected, since partial isolation is increasing the overall displacement demands of the bridge. The acceptable abutment displacement or ductility demand under this approach is at the discretion of the designer, but very large demands, on the order of 2-3 times larger than in a conventional bridge, are probably unacceptable.

Abutment displacement ratio $u_a / u_{a,con}$ for both linear and nonlinear partial isolation increases with increasing α_k for a fixed T_{iso} and also increases with increasing T_{iso} for a fixed α_k. T_{iso}=1 sec is very effective in limiting the abutment displacements; for periods T_{iso}>2 sec the effect of the period is small.

Overall the abutment displacement ratio is generally larger for linear isolation than nonlinear isolation because it has a smaller effective damping ratio (Figure 3.4). Appropriately, increasing the effective damping ratio reduces the displacement demand of the abutment, but the overall increase in bridge displacement that underlies the concept of response modification using isolation devices is inevitably passed to the abutments if they are not isolated.

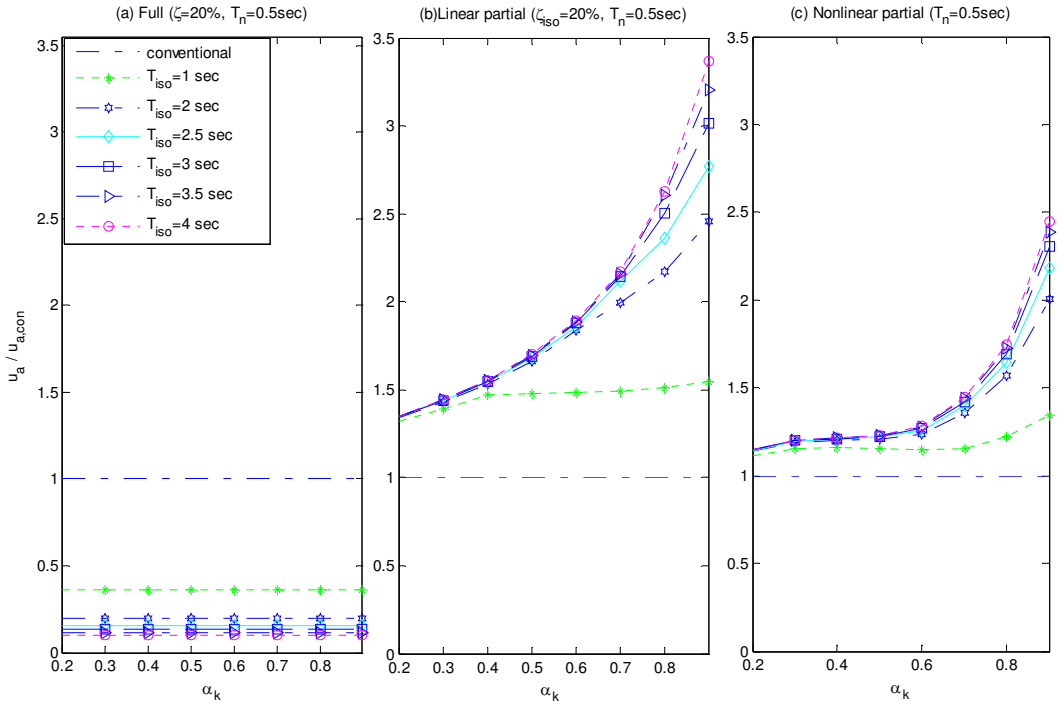

Figure 4.6 (a) - (b) $u_a / u_{a,con}$ vs. α_k for different isolation systems.

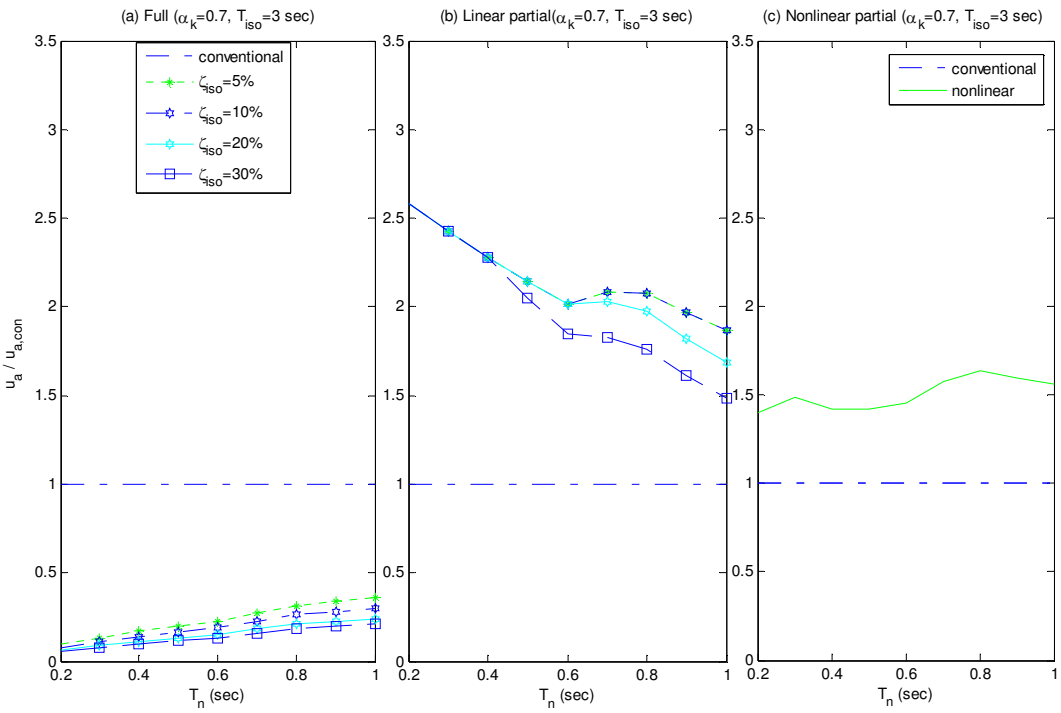

Figure 4.7 (a) - (c) $u_a / u_{a,con}$ vs. T_n for different isolation systems.

Finally, Figures 4.8 and 4.9 present the force demands of the abutments relative to a conventional bridge ($F_{y,a} / F_{y,a(con)}$) for different isolation options. Since the distribution of abutment forces is unaffected by full isolation, the abutment force ratio of the fully isolated bridge is identical to the column force ratio of the fully isolated bridge (Figure 4.8(a), 4.9(a) vs. Figure 4.4(a), 4.5(a)). For linear partial isolation, the force demands of the abutments are not reduced below the force demands of the conventional bridge over any range of parameters. The abutment force decreases as the stiffness and strength distribution shifts from the abutments to the columns (α_k increases) (Figure 4.8(b)). The abutment force decreases rapidly with increasing period up to about T_n=0.5 sec, and then decreases more moderately thereafter (Figure 4.9(b)). The yield force of the abutment for nonlinear partial isolation is the same as that of a conventional bridge as imposed by the design procedure (Figure 4.8(c) and Figure 4.9(c)).

In summary, Figures 4.1-4.9 have shown that a linear partial isolation is not an effective strategy because it generally increase force demands in both the columns and abutments. On the other hand, nonlinear partial isolation can be effective to reduce the force and displacement demands of the columns and abutments in certain parameter ranges. For larger α_k (>0.5) and larger T_n (>0.4sec), the effectiveness of nonlinear partial isolation is close to full isolation for reducing the yield force and displacement of columns. However, the displacement demands of the abutments in the partial isolation can not be reduced. While the isolation period has little influence on column displacements and forces, a smaller isolation period may be an effective strategy to minimize abutment displacements.

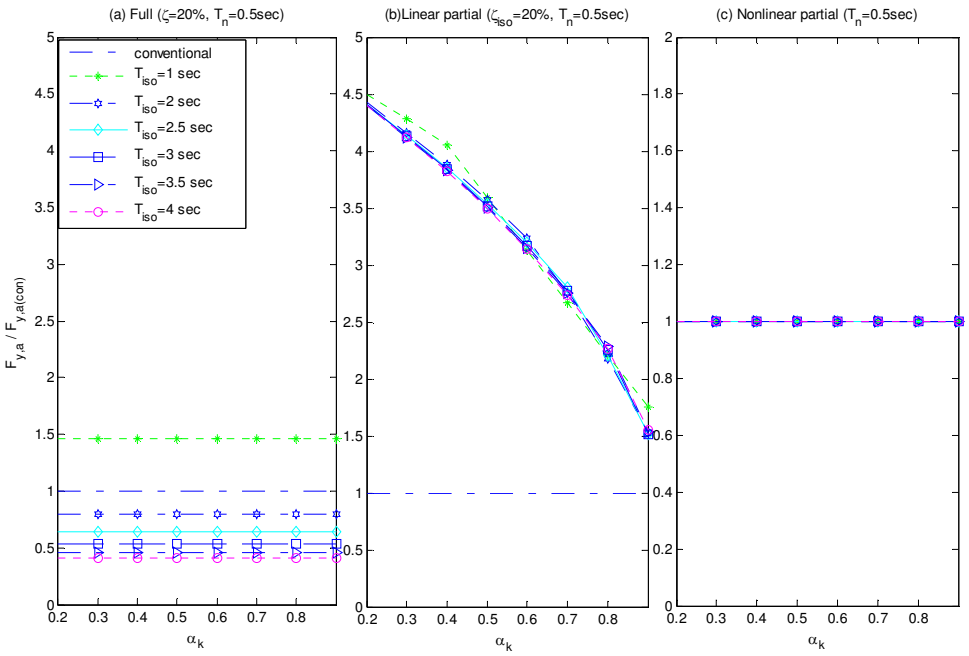

Figure 4.8(a) - (c) $F_{y,a} / F_{y,a(con)}$ vs. α_k for different isolation systems.

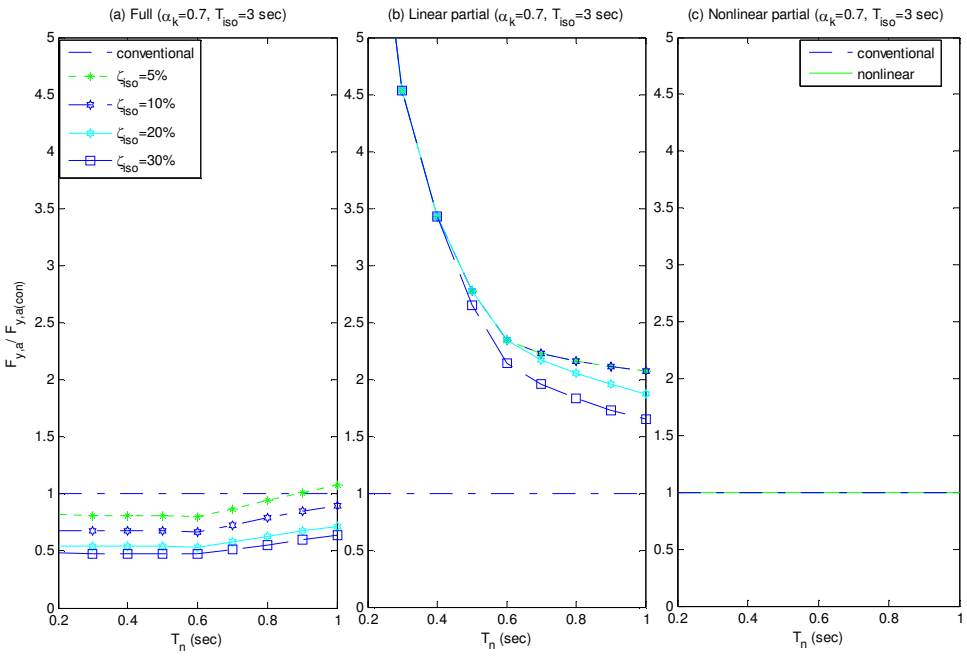

Figure 4.9(a) - (c) $F_{y,a} / F_{y,a(con)}$ vs. T_n for different isolation systems.

Partial isolation may be viewed as being effective if the performance of the columns is viewed as being more critical to the life safety of the bridge; that is, a bridge is unlikely to collapse due to abutment failure. The strategy of nonlinear partial isolation is investigated further through response history analysis.

CHAPTER 5

VERIFICATION BY RESPONSE HISTORY ANALYSIS

In this chapter, the peak response of partially isolated bridges is computed by time history analysis using OPENSEES, and compared to the response using static analysis, as validation of the simplified static evaluation procedure for nonlinear partial isolation. Time history analysis results are compared to static analysis results for conventionally and fully isolated bridges as well.

5.1 Ground Motions to Simulate the Design Spectrums

Ground motions are selected to be representative of the design spectrum used for conventional and isolated bridge (Figure 3.1). Spectrum-compatible time histories may be generated by scaling recorded ground motions of past earthquakes such that their spectra closely match the design spectral amplitude for the site at a given natural period. An ensemble of 20 motions has been selected for this study, which were originally generated for the SAC Steel project. The motions represent a 2% in 50-year probability of exceedance for the Los Angeles region, which is seismically similar to Salt Lake City. The median displacement spectrum of the SACLA 2 in 50 ensembles is plotted along with the design spectrum for conventional (Figure 5.1 (a)) and isolated bridges (Figure 5.2 (a)).

Based on the difference between the design and SAC LA displacement spectrum (Figure 5.1 (b) and Figure 5.2(b)), the motions are scaled by a period dependent amplification factor (Table 5.1) so that the median spectrum of the ground motion histories matches the design spectral displacement for each natural period.

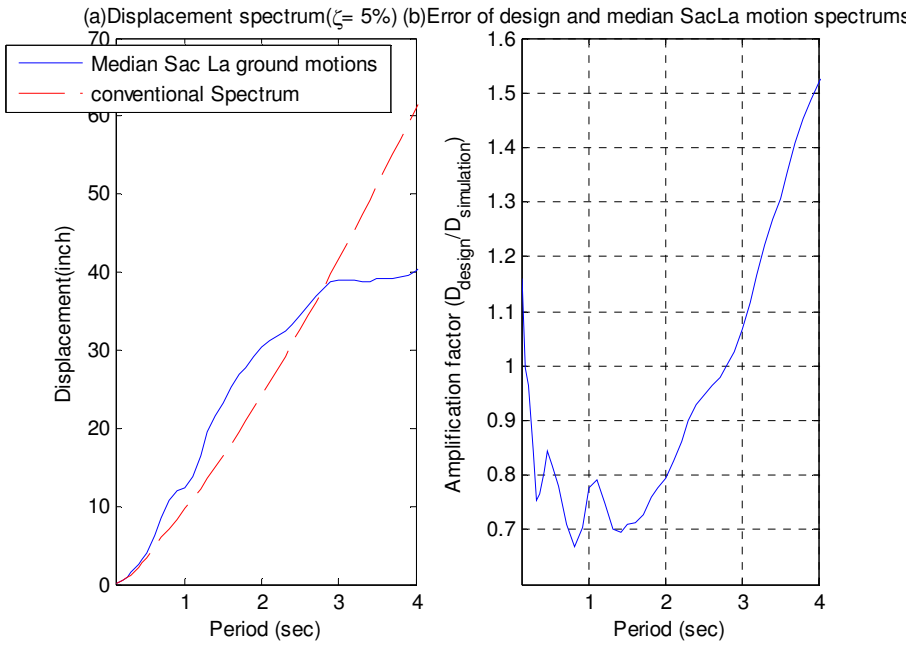

Figure 5.1(a) and (b) Comparison of median spectrum and conventional design spectrum.

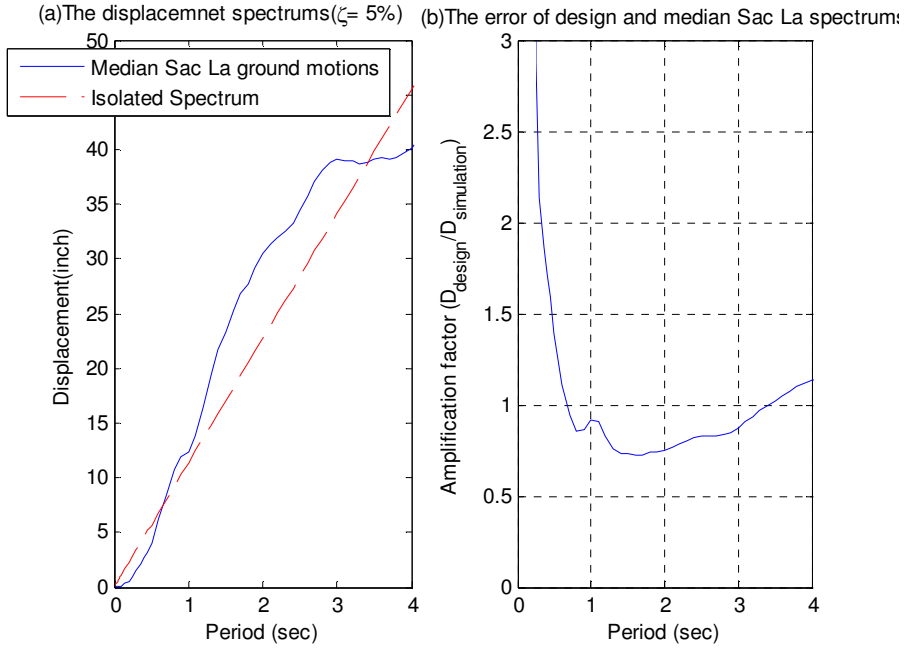

Figure 5.2(a) and (b) Comparison of median spectrum and isolated design spectrum.

Table 5.1 Amplification factor for different base conditions

Period (sec)	Amplification factor	
	conventional	isolated
0.1	1.1589	-
0.2	0.96425	-
0.3	0.7538	-
0.4	0.8072	-
0.5	0.81892	-
0.6	0.77958	-
0.7	0.70862	-
0.8	0.66952	-
0.9	0.70237	-
1	0.77657	0.9182
1.1	0.79055	0.90551
1.2	0.74664	0.83076
1.3	0.70061	0.75902
1.4	0.69642	0.73607
1.5	0.71009	0.73346
1.6	0.71158	0.71935
1.7	0.72758	0.72082
1.8	0.75934	0.73809
1.9	0.77715	0.7419
2	0.79554	0.74659
2.1	0.82724	0.76381
2.2	0.86286	0.78444
2.3	0.89873	0.80503
2.4	0.92829	0.81979

Table 5.1 (continued)

2.5	0.9473	0.82528
2.6	0.96399	0.82891
2.7	0.97739	0.82992
2.8	0.9979	0.83713
2.9	1.0262	0.85086
3	1.0655	0.87355
3.1	1.1154	0.90452
3.2	1.1667	0.93616
3.3	1.2214	0.96998
3.4	1.2673	0.99648
3.5	1.3071	1.0179
3.6	1.354	1.0446
3.7	1.4072	1.0757
3.8	1.4521	1.1002
3.9	1.488	1.1177
4	1.5201	1.1323

5.2 OPENSEES Model Description for History Analysis

A simple mass-spring model of each bridge is developed in OPENSEES for response history analysis. For each bridge, the total mass of the bridge is lumped on top of a spring assemblage that represents the particular combination of column, abutment, and isolator elements.

For the conventional bridge, two springs are assembled in parallel to represent the substructure (column and abutment) and a linear dashpot that provides 5% damping

(Figure 5.3). The substructure spring has elastic-perfectly plastic behavior as provided by the material model.

For the fully isolated bridge, a spring representing the isolation system is assembled in series with the spring assemblage representing the conventional bridge (Figure 5.4). The isolation spring is linear which also represents the damper of the isolator (ζ=5%, 10%, 20%, 30%), while the substructure element is elastic-perfectly plastic. As before, an additional linear dashpot is added to the substructure to represent the 5% viscous damping.

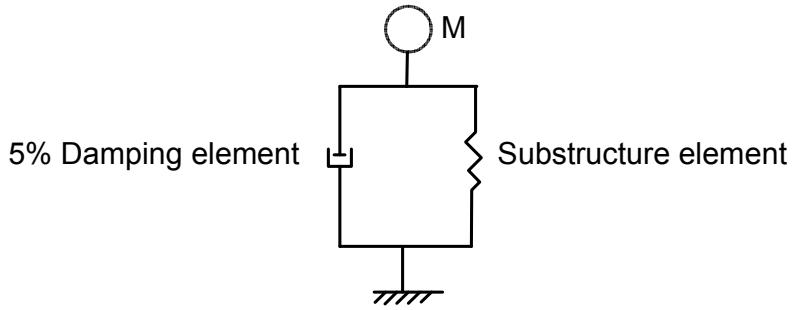

Figure 5.3 Model of conventional bridge.

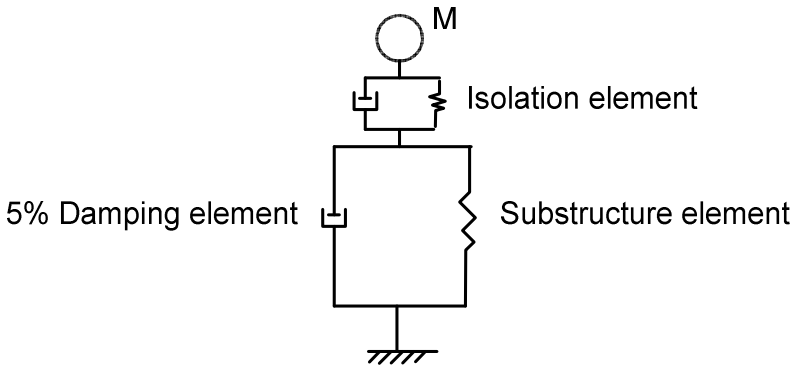

Figure 5.4 Model of full isolation system.

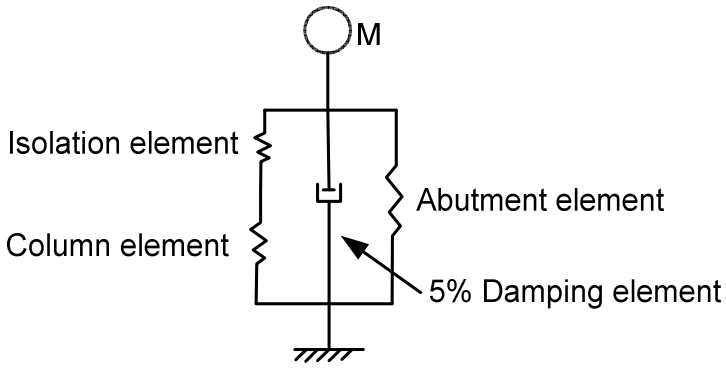

Figure 5.5 Model of nonlinear partial isolation system.

For the nonlinear partially isolated bridge, springs representing the isolator and column are assembled in series, and in parallel with the abutment (Figure 5.5). Because the yield force of the column is 10% greater than the yield force of the isolator, the column can never yield and is kept elastic in this model. The spring representing the isolation system and the abutment are elastic-perfectly plastic. A linear dashpot is again added to the whole bridge to represent the 5% viscous damping.

5.3 Comparison of the Results for the Static and History Analysis

Response history analysis to the SAC LA ensemble of motions scaled as described previously is performed for each of the bridges. The peak deformation and force in each element for each ground motion is recorded. The peak response $\overline{x}$ is generated by computing the geometric mean on the individual observations x_i:

$$\overline{x} = \exp(\sum_i \ln(x_i) / 20) \tag{5.1}$$

In this section, resulting displacement demands from the static (u_c or u_a) and response history analysis ($u_{c,h}$ or $u_{a,h}$) are compared. These comparisons indicate

the accuracy of the static analysis for different bridge models. The static and history analysis results are compared for conventional and isolated bridges as a reference for interpreting the comparable comparisons for partially isolated bridges.

For a conventional bridge, the displacement estimated by static analysis is generally reasonably accurate, i.e. for T_n> 0.4sec the static displacement is within 20% of the median displacement determined by history analysis (Figure 5.6). Certainly, the equations that account for strength and ductility (Equation (3.10)) have been well established.

The static analysis method appears to be very unconservative for a fully isolated bridge (Figure 5.7), especially for long isolation periods or short superstructure periods where isolation is expected to reduce displacement demands to essentially zero.

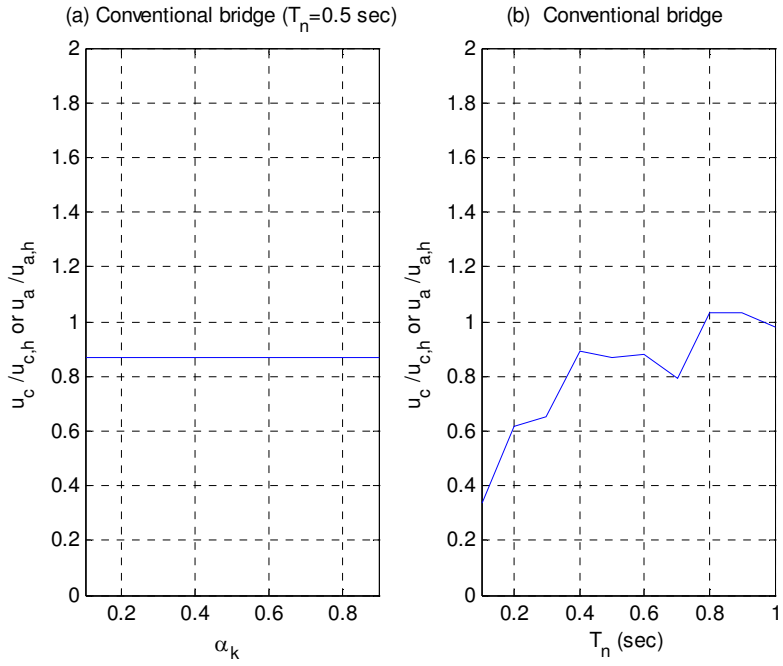

Figure 5.6 Comparison of the static and response analysis for conventional bridge.

The observed behavior is a result of substructure yielding that is not accounted for in the static analysis. Since the motions have been scaled to match the design spectrum on average, substructure yielding is expected to occur approximately 50% of the time (whenever the ground motion exceeds the design spectrum).

Compared to full isolation, static analysis of partially isolated bridge gives much better results over a large range of parameters. The ratio of abutment displacements determined by static analysis and history analysis ($u_a / u_{a,h}$) varies from 0.8 to 2.6 (Figure 5.8(a) and (b)). When the column stiffness ratio (α_k) is greater than 0.4 or T_n is greater than 0.4 sec, which represents the parameter range where partial isolation is most effective, the ratio is close to 1. The ratio of column displacements determined by static analysis and history analysis ($u_c / u_{c,h}$) varies from 0.7 to 1 (Figure 5.8(c) and (d)). Thus, column displacements estimated by static analysis are more accurate for partial isolation than for full isolation, but still tend to be unconservative compared to a history analysis.

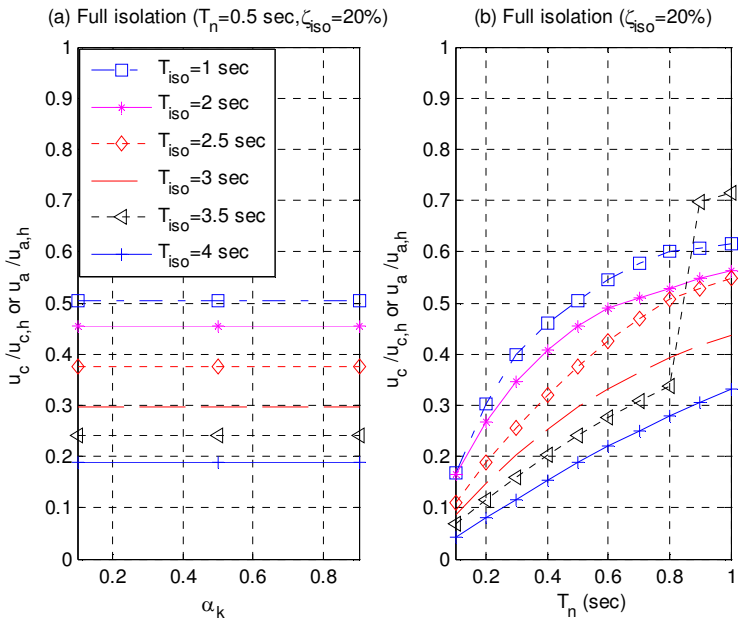

Figure 5.7 Comparison of the static and response analysis for fully isolated bridge.

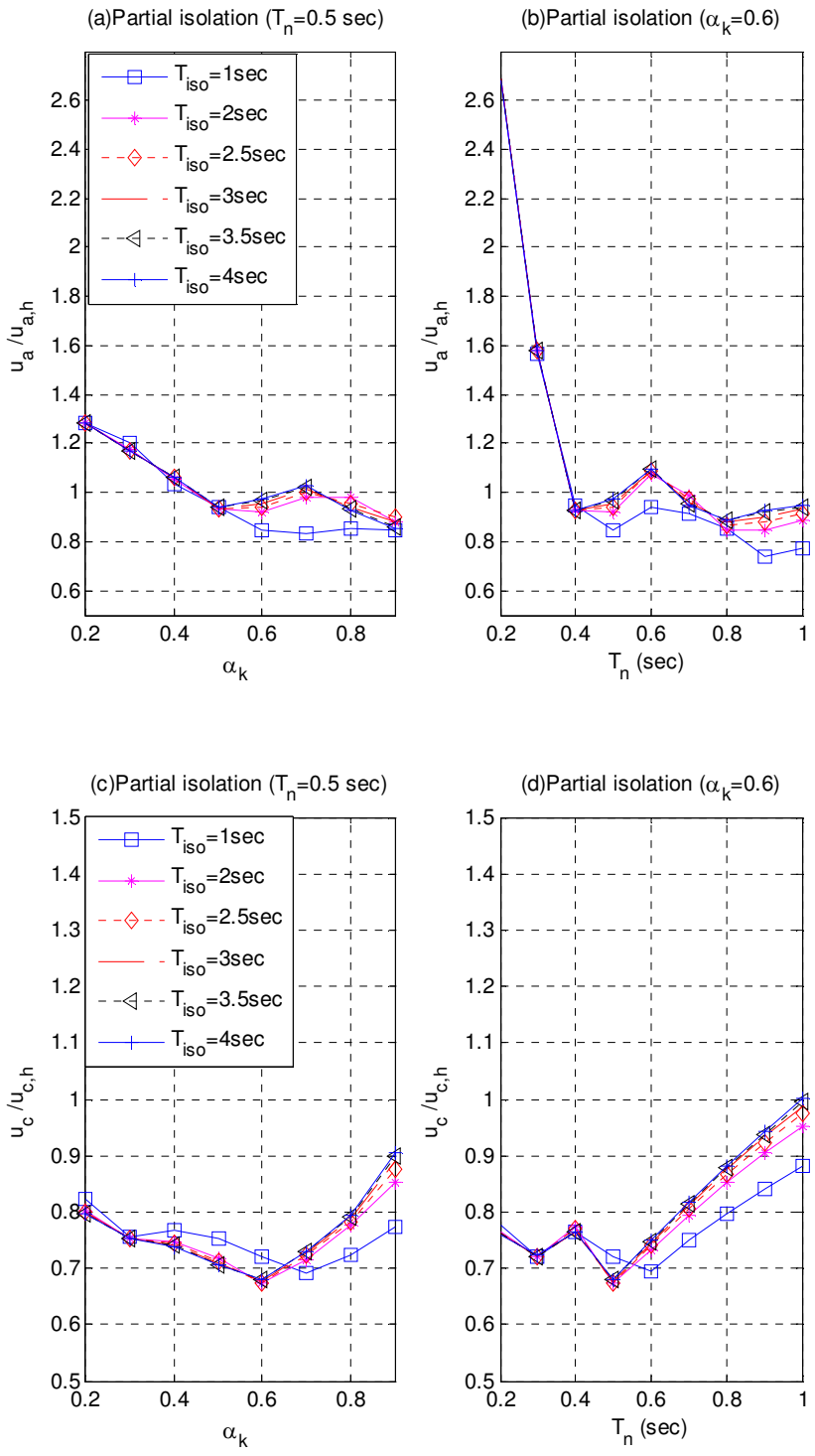

Figure 5.8 (a)-(d) Comparison of static and response analysis for partial isolated bridge.

In summary, we conclude that the static analysis procedure developed here for partially isolated bridges is more accurate than the established procedure for fully isolated bridge but not as accurate as the established procedure for conventional bridges. Because a procedure has not completely been established for partially isolated bridge, the evaluation procedure proposed here should be used for preliminary evaluation only.

CHAPTER 6

PRACTICAL EXAMPLE

6.1 Properties and Modeling of the Conventional Bridge

In this chapter, a representative bridge in the state of Utah is chosen to demonstrate the partial isolation approach developed in the previous chapters.

The bridge is a hypothetical 2-span continuous reinforced concrete that is representative of a typical freeway overcrossing. Each span is 130 ft and the length of the whole bridge is 260 ft. The superstructure consists of an 7.5" thick (46'-10" wide) reinforced concrete slab supported on four rectangular reinforced concrete girders spaced at 10'- 8". The total weight of the superstructure is 3318 kips. The superstructure is fixed in the transverse direction and in the longitudinal direction at each of the two piers. The abutments are integral. The center pier is a two-column bent with identical 4' diameter circular reinforced concrete columns. Each column is fixed (Figure 6.1).

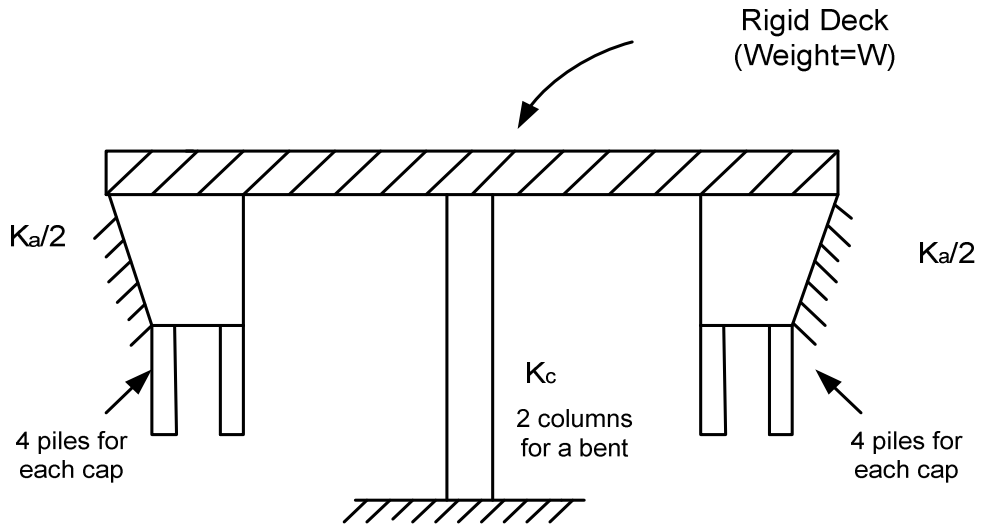

Figure 6.1 Two spans bridge model.

The stiffness and strength of the abutments are estimated based on the passive pressure of the surrounding soil. The soil type in this problem is close to sand; thus 2H/3 is used for passive pressure. The effects of the piles beneath the abutment are also included in abutment stiffness, which leads to:

$$P_p = p_p.H.L + N_p.C_p \tag{6.1}$$

where P_p is the total lateral capacity of the abutment-pile system, H is the height of the abutment, p_p is the passive pressure, L is the width of the backwall, N_p is the number of piles, and C_p is the capacity of each pile. The piles are assumed to yield when the soil reaches its passive pressure. The displacement at which soil reaches to its passive pressure is called mobilization displacement, recommended to be $0.02H$ (Buckle et al., 2006b). Thus, the effective stiffness is:

$$K_{eff} = \frac{P_p}{0.02H} \tag{6.2}$$

For this bridge, the width of the backwall L is 46'10'', the height of abutment H is 6 ft, and the capacity of each pile is 40 kips. When the bridge moves longitudinally, one abutment is in compression and the other is in tension. The compression and tension capacity of each abutment-pile system in the longitude direction is

$$P_{p\_long\_com} = p_p.H.L + N_p.C_p$$

$$= 46.8333 \cdot 6 \cdot (2/3 \cdot 6) + 4 \cdot 40$$

$$= 1284 \text{ kips} \tag{6.3}$$

$$P_{p\_long\_ten} = N_p.C_p = 160 \text{ kips} \tag{6.4}$$

$$K_{a\_long\_com} = \frac{1284}{0.02 \cdot 6} = 10700 \text{ kips/ft} \tag{6.5}$$

$$K_{a\_long\_ten} = \frac{160}{0.02 \cdot 6} = 1333.3 \text{ kips/ft} \tag{6.6}$$

A similar procedure is applied in the transverse direction, but the transverse stiffness of the abutment is provided by wing walls. It is proposed to take the effective width as the length of the wing walls multiplied by a factor of 8/9 to account for differences in participation of both wing walls (Priestley, Seible and Calvi, 1996). Given a wingwall width of 15 ft, the compression capacity of each abutment-pile system in the transverse direction is

$$P_{p\ \ wingwall} = \frac{2}{3} \cdot \frac{8}{9} \cdot 6^2 \cdot 15 = 320 \quad kips \tag{6.7}$$

$$P_{p\ \ piles} = 4 \times 40 = 160 \quad kips \tag{6.8}$$

$$P_{p\_trans} = 320+160 = 480 \text{ kips} \tag{6.9}$$

$$K_{a\_trans} / 2 = \frac{480}{0.02 \cdot 6} = 4000 \quad kips / ft \tag{6.10}$$

The assumed column diameter is 4 ft and the height is 15 ft. A 1% steel ratio is assumed, and typically large reinforcement bars (#9 or #11) are selected. Based on these parameters, the gross area of each column is $\frac{\pi}{4} D^2 = \frac{\pi}{4} 4^2 = 12.5664$ ft^2, the area of the steel is $0.01 \cdot 12.5664 = 0.125664 ft^2 = 18.0956\ in^2$. Assuming #11 bars (with area = 1.56 in^2), 12 bars are needed for each column.

Ultimate moment capacities for the columns are obtained from the computer generated column interaction diagrams. Moment capacities depend on axial loads while axial loads in turn depend on moment capacities. The shear force V_n sustained by each column is given by:

$$V_n = \frac{M_n}{H} \tag{6.11}$$

where H is the height of the column, assuming 15ft, M_n is the moment capacity on one side of column. Wherein the total dead load of the deck is 3318.2 kips, each column carries about 531.3 kips axial load. Determined from computer analysis, the capacity of each column (M_n) is about 27648 kips.in. From Equation 45, the shear force of each column V_n=153.6 kips, so the corresponding total yield force of the columns is $F_{y,c}$ = $2V_n$=307.2 kips.

The effective flexural rigidity of a severely cracked structural concrete column (Buckle et al., 2006b) is:

$$E_c I_{eff} = \frac{M_n D'}{2\varepsilon_Y} \tag{6.12}$$

where D' is the distance between outer layers of longitudinal reinforcement, and $\varepsilon_y = f_y / E_s$ is the yield strain of steel reinforcement.

$$D' = 48\text{-}3\text{-}1 = 44\ in \tag{6.13}$$

$$f_y = 36ksi \tag{6.14}$$

$$\varepsilon_y = 36/30000 = 0.0012 \tag{6.15}$$

$$E_c I_{eff} = \frac{27648 \cdot 44}{2 \cdot 0.0012} = 5.0688 \times 10^8 \tag{6.16}$$

The stiffness of each column is:

$$K_c / 2 = \frac{12 E_c I_{eff}}{L^3} = 1043 kips/in = 12516 kips/ft \tag{6.17}$$

The total stiffness (K), stiffness and yield force distribution of columns, displacement and period of the whole bridge (T_n) in both directions should be:

$$K_{a\_long} = K_{a\_long\_ten} + K_{a\_long\_com} = 10700 + 1333.3 = 12033.3 kips / ft \quad (6.18)$$

$$K_{long} = K_c + K_{a\_long} = 12516 * 2 + 12033.3 = 37065 kips / ft \quad (6.19)$$

$$K_{trans} = K_c + K_{a\_trans} = (12516 + 4000) \cdot 2 = 33032 kips / ft \quad (6.20)$$

$$\alpha_{k\_long} = K_c / K_{long} = 12516 \cdot 2 / 37065 = 0.6754 \quad (6.21)$$

$$\alpha_{k\_trans} = K_c / K_{trans} = 12516 \cdot 2 / 33032 = 0.7578 \quad (6.22)$$

$$F_{y,a\_long} = P_{p\_long\_com} + P_{p\_long\_ten} = 1284 + 160 = 1444 kips \quad (6.23)$$

$$F_{y,a\_trans} = 2P_{p\_trans} = 960 kips \quad (6.24)$$

$$\alpha_{F\_long} = F_{y,c} / (F_{y,c} + F_{y,a\_long}) = 614.4 / (614.4 + 1444) = 0.2985 \quad (6.25)$$

$$\alpha_{F\_trans} = F_{y,c} / (F_{y,c} + F_{y,a\_trans}) = 614.4 / (614.4 + 960) = 0.3902 \quad (6.26)$$

$$T_{n\_long} = 2\pi \sqrt{\frac{m}{K_{long}}} = 0.3315 \sec \quad (6.27)$$

$$T_{n\_trans} = 2\pi \sqrt{\frac{m}{K_{long}}} = 0.3509 \sec \quad (6.28)$$

$$u_{long} = 2.857 inch \quad (6.29)$$

$$u_{transs} = 3.055 inch \quad (6.30)$$

Based on the previous calculations, 3D renderings of the bridge model, created using the SAP2000 software, are shown in Figure 6.2.

Three uncoupling springs represent each abutment elements: tension capacity is 1284 kips and compression capacity is 160 kips, yield displacement is 0.12 ft for

horizontal translate spring in longitude direction; in the transverse direction both tension and compression capacity is 480 kips, and yield displacement is also 0.12 ft; the rotation spring about the vertical direction should be $(L^2/12)K_{long}$, and L is the width of the back wall. Here the spring about vertical direction is assumed be linear 731120 kips.ft.

The deck is rigid compared with the substructures. By static analysis, the total weight of this conventional bridge (W) is 3318 kips. By eigenvalue analysis using SAP2000, the natural period is 0.37216 *sec* in the longitude direction, and 0.39523 second in the transverse direction, which are slightly longer than the periods estimated by hand calculations. The maximum displacement of the substructure estimated according to the updated periods is 2.756 inches in the longitude direction and 3.147 inches in the transverse direction, which represents only a minor change.

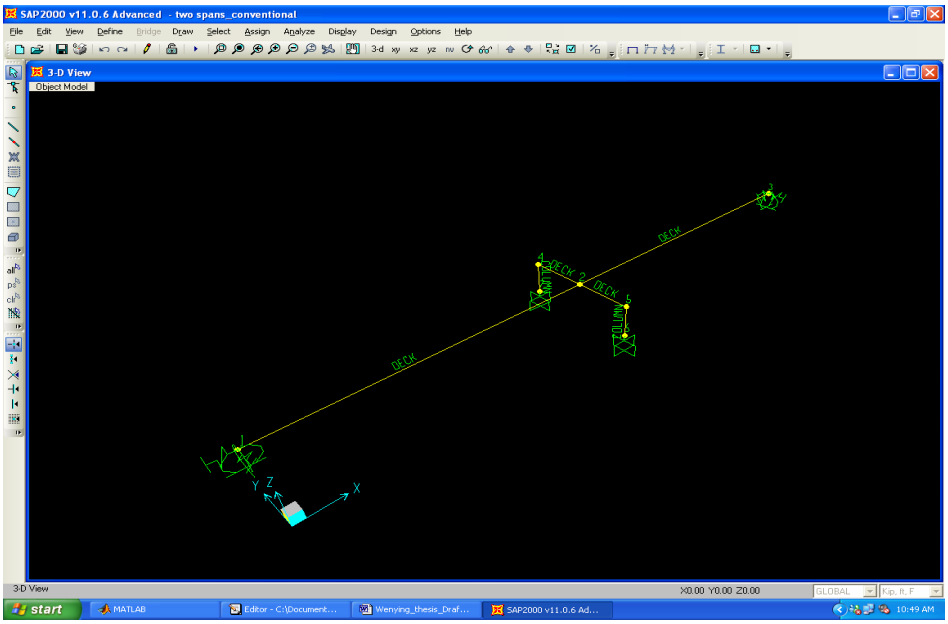

Figure 6.2 SAP2000 model of the conventional bridge.

6.2 Modeling and Analysis of the Nonlinear Partially Isolated Bridge

Next, nonlinear partial isolation is applied to this existing bridge model by adding isolators at the abutments, and the bridge is analyzed by response history analysis using SAP 2000. The response history analysis of the partially isolated bridge using a more realistic model provides an additional check of the results computed by static analysis.

Table 6.1 shows the properties of the partially isolated bridge based on the static design procedure of nonlinear partial isolation.

Table 6.1 Properties of nonlinear partially isolated bridge

Parameters	Direction	
	Longitude	Transverse
T_n (sec)	0.37216	0.39523
α_k	0.591	0.693
T_{iso} (sec)	3	3
T_{eff} (sec)	0.575	0.700
ζ_{eff} (%)	5	6.808
$F_{y,}$ (kips)	1916.231	1450.92
$F_{y,a}$ (kips)	1444	960
u_a (inch)	5.284	6.287
$F_{y,iso}$ (kips)	472.231	490.92
u_{iso} (inch)	5.61	5.961
$F_{y,c}$ (kips)	519.455	540.012
u_c (inch)	0.326	0.326

The periods T_n and column stiffness ratios α_k represent the updated values from eigenvalue analysis of the conventional bridge. An isolation period of Tiso = 3 seconds is assumed, and the effective periods are estimated by hand calculation 0.644 sec in the longitudinal direction and 0.782 seconds in the transverse direction. The required isolator yield force $F_{y,iso}$ is computed by subtracting $F_{y,a}$ for the conventional bridge from the new F_y.

The SAP2000 model of the partially isolated bridge is created by adding elastic plastic springs between the superstructure and columns to represent the isolators (Figure 6.3). Because the isolator is a bidirectional coupled element with the same yield force in each direction, we select the isolator properties based on the larger value $F_{y,iso}$ = 490.92 kip in the transverse direction, which ensures that a force reduction factor of no more than 3 in each direction. The yield force of each isolator is 245.46 kips and yield displacement is 0.1 cm. The column element is assigned to be elastic since the column is guaranteed not to yield. The coefficient of friction of the elastic plastic slider is $\mu = F_{y,iso}/W_{iso}$ =245.46/531= 0.4, which may be higher than a typical slider can provide. Figure 6.4 illustrates representative force-deformation behavior of the isolator element, where the bidirectional coupling is apparent through the circular interaction surface shown in the plot of F_x versus F_y.

The bridge is analyzed again using the SACLA 2 in 50 suites of motions, which are now grouped into ten orthogonal pairs. A single scale factor (0.793) is applied to the entire set of motions, which is determined by minimizing the least square difference of the median spectrum and the design spectrum over the period range of 0.1 to 3 seconds.

A single scaling factor is chosen, rather than a period dependent scaling factor, because the actual period of the bridge is more complex to determine.

Figure 6.4 illustrates representative force-deformation behavior of the isolator element, where the bidirectional coupling is apparent through the circular interaction surface shown in the plot of F_x versus F_y.

Table 6.2 lists the maximum isolator, abutment and column displacements for each pair of motions, and also tabulates the median values. For the partially isolated bridge, the median displacements of isolator and abutment are larger than those predicted by static analysis, and the median displacements of column are smaller. Comparing with the SAP2000 results of conventional bridge, the displacement of abutment increases and the displacement of column decreases, which are consistent with the static design procedures.

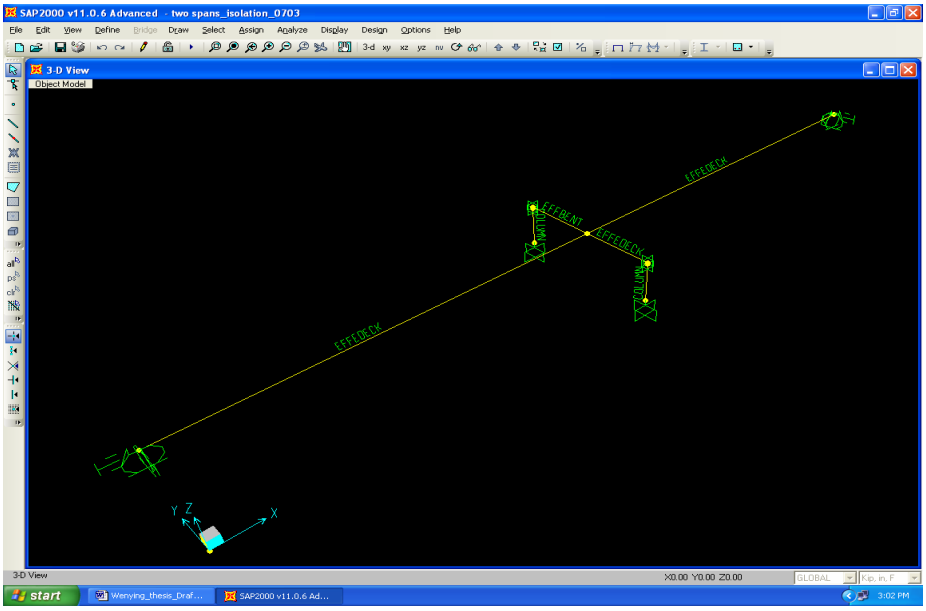

Figure 6.3 SAP2000 model of the partially isolated bridge.

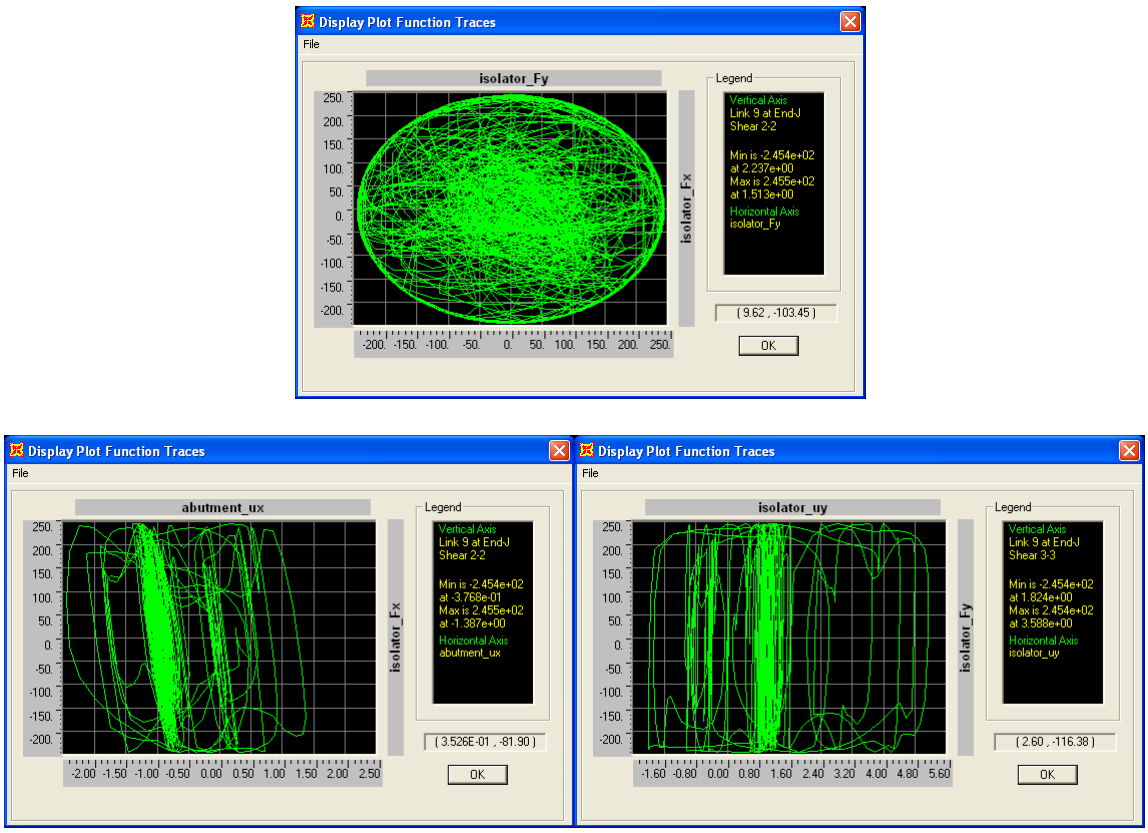

Figure 6.4 Force deformation capacity curve of isolator resulting from SAP2000.

Table 6.2 Results of SAP2000 analysis for the partially isolated bridge

motion	u_{iso} (inch)		u_c (inch)		u_a (inch)	
	longitude	transverse	longitude	transverse	longitude	transverse
1	17.88	10.71	0.13	0.13	17.87	10.59
2	2.12	4.28	0.13	0.13	2.133	4.28
3	8.827	11.02	0.13	0.13	8.837	10.88
4	6.716	6.38	0.13	0.13	6.725	6.352
5	2.454	5.04	0.13	0.13	2.455	5.034
6	5.515	10.66	0.13	0.13	5.524	10.44
7	3.201	5.15	0.13	0.13	3.21	5.128
8	11.71	11.4	0.13	0.13	11.72	11.4
9	5.433	13.24	0.13	0.13	5.424	13.29
10	1.916	4.6	0.13	0.13	1.925	4.678
average	6.5772	8.248	0.13	0.13	6.5823	8.2072

Because the column force demands are reduced through partial isolation, the bridge columns should be redesigned to see a savings in material costs and also foundation demands. Because a redesign of the columns would affect their stiffness, iteration would be required to determine the final response of the bridge. This design iteration is not performed here.

CHAPTER 7

CONCLUSION

This study to evaluate the effectiveness of the partial isolation in the bridges has led to the following conclusions:

1. In the static analysis of partial isolation systems, two kinds of isolation systems were proposed: linear and nonlinear isolations. Although linear partial isolation reduces the displacement demand of the columns, the force demands of the columns and abutments are always increased due to the smaller force reduction factor. Nonlinear partial isolation effectively reduces the displacement demand of the columns and for some parameters the force demand of the columns can also be reduced. In addition, the force demand of the abutments is the same as for a conventional bridge, leading to higher abutment ductility demands. Nonlinear partial isolation is an effective technique that can be considered if lowering columns demands is a high priority, and some performance in the abutments can be sacrificed.
2. Full isolation is a very useful way to reduce the effect of the earthquake and accepted widely. Nonlinear partial isolation was shown to perform as effectively as full isolation to reduce the demand of the columns when the natural period of the substructure and the column stiffness ratio are large. For retrofit applications where the abutment connections are integral, making full isolation impractical, partial isolation may be a cost effective way to reduce the demands on the columns.

3. Compared to a fully isolated bridge, the partially isolated bridge performance is not that sensitive to the isolation period. A very large isolation period does not improve the performance of the bridge, where a smaller isolation period limits abutment displacement demands.
4. The partial isolation system cannot effectively reduce the displacement demand of the abutments under any circumstances. Thus, improvement of the ductility capacity of the abutments is an added consideration.
5. Response history analysis in OPENSEES induced similar response of the bridge as predicted by static analysis to the design spectrum. From the results of the time history analysis, the static analysis procedure for nonlinear partial isolation is a reliable first approximation.

One of the key questions this study has tried to solve is if the partial isolation technique is an effective way to improve the response of the bridge during an estimated earthquake.

Requiring the isolation devices in partial isolation to elastic-plastic guarantees reduced yield force and displacement of the columns. These types of devices are not preferred for full isolation, because the displacement demands are large and uncertain, but the abutment stiffness limits the displacement demands for a partially isolated bridge. Unfortunately, the approach causes excessive ductility demand of the abutments, which is a challenge to be dealt with for realistic application. The information in this study is a starting point for future investigation to apply the concept to more realistic bridges with complex abutment and foundation force- deformation behavior, as well as transverse/longitudinal effects.

REFERENCES

AASHTO. 1999. *Guide specifications for seismic isolation design*, second edition, American Association of State Highway and Transportation Official, Washington, D. C.

AASHTO. 2002. *Standard specifications for highway bridges.* American Association of State Highway and Transportation Official, Washington, D. C.

Boroschek, R. L., María O. Moroni, and Mauricio Sarrazin. 2003. *Dynamic characteristics of a long span seismic isolated bridge*. Engineering Structures 25 (12): 1479-1490.

Buckle, I.G., Michael C. Constantinou, Mirat Diclli, and Hamid Ghasemi. 2006a. *Seismic isolation of highway bridges*. MCEER Publications, State University of New York, Buffalo. 171 p.

Buckle, I., Iran Friedland, John Mander, Geoffrey Martin, Richard Nutt, and Maurice Power. 2006b. *Seismic retrofitting manual for highway structures: Part 1-bridges.* MCEER Publications, State University of New York, Buffalo. 583 p.

Chopra, A. K. 2000. *Dynamics of structures: Theory and applications to earthquake engineering. Second ed.* Prentice Hall, Upper Saddle River, NJ. 844 p.

Constantinou, M. C., and Joseph K. Quarshie. 1998. *Response modification factors for seismically isolated bridges*. MCEER Publications, Buffalo, 92 p.

Friedland, I. M., Ronald L. Mayes, and Michel Bruneau. 2001. *Recommended changes to the AASHTO specifications for the seismic design of highway bridges.* Report on Progress and Accomplishments: 2000-2001. MCEER Publications, State University of New York, Buffalo. P. 41-50.

Lee, G. C., Yasuo Kitane, and Ian G. Buckle. 2001. *Literature review of the observed performance of seismically isolatedBridges.* Report on Progress and Accomplishments: 2000-2001, MCEER Publications, State University of New York, Buffalo. P. 51-61.

Priestley, M.J.N. F., Seible, and G.M. Calvi. 1996. *Seismic design and retrofit of bridges.* John Wiley & Sons, Inc., New York, 686p.

Shen, J., Meng-Hao Tsai, Kuo-Chun Chang, and George C. Lee. 2004. *Performance of a seismically isolated bridge under near-fault earthquake ground motions*. Journal of Structure Engineering, 130(6): 861-868.

Tsopelas, P., and Michael C. Constantinou. 1997. ASCE *study of elastoplastic bridge seismic isolation system.* Journal of Structure Engineering, 123(4): 489-498.